Size-dependent behaviour of functionally graded microbeams using various shear deformation theories based on the modified couple stress theory

Luan C. Trinh[a,b], Hoang X. Nguyen[a], Thuc P. Vo[a,*], Trung-Kien Nguyen[b]

[a]*Faculty of Engineering and Environment, Northumbria University, Newcastle upon Tyne, NE1 8ST, UK.*
[b]*Faculty of Civil Engineering and Applied Mechanics, Ho Chi Minh City University of Technology and Education, 1 Vo Van Ngan Street, Thu Duc District, Ho Chi Minh City, Vietnam*

Abstract

This study investigates the mechanical behaviours of functionally graded (FG) microbeams based on the modified couple stress theory. The material properties of these beams are varied through beam's depth and calculated by using classical rule of mixture and Mori-Tanaka scheme. The displacement fields are presented by using a unified framework which covers various theories including classical beam theory, first-order beam theory, third-order beam theory, sinusoidal beam theory, and quasi-3D beam theories. The governing equations of bending, vibration and buckling problems are derived using the Hamilton's principle and then solved by using Navier solutions with simply-supported boundary conditions. A number of numerical examples are conducted to show the validity and accuracy of the proposed approaches. Effects of Poisson's ratio, material length scale parameter, power-law index, estimation methods of material properties and slenderness ratio on deflections, stresses, natural frequencies and critical buckling loads of FG microbeams are examined.

Keywords: Functionally graded microbeams, modified couple stress theory, bending, buckling, vibration

1. Introduction

Functionally graded materials (FGM) are increasingly used in the many fields of industrial engineering including automotive, nuclear power plant, aerospace. Basically, FGMs could be consider as a class of composite material which contains two or more constituents varying continuously from a surface to the other. This smooth variation of phases enables the material to avoid stress concentration and delamination phenomenon which are often cited as the shortcomings of laminated fiber composite materials. High attention is being paid in the researcher community to investigate the behaviours of

*Corresponding author, tel.: +44 191 243 7856
Email address: thuc.vo@northumbria.ac.uk (Thuc P. Vo)

structures made of FGMs such as beams, plates, and shells ([1–3]).

The development of technology leads to the trend in which structural elements become smaller and smaller in their dimension. The small-scale elements are now used in the variety of areas such as micro- and nano-electro-mechanical system [4], actuators [5]. This growing trend has attracted huge attention from the researcher to study the behaviours of small-scale structures. It is known that those responses are size-dependent ([6–8]) which the classical theories of mechanic are failed to capture. Some mechanical theories have been proposed to consider size-dependent effects such as nonlocal elasticity theory [9], strain gradient theory [10], micropolar elasticity ([11, 12]) and modified couple stress theory [13]. Among those, the modified couple stress theory is considered as a prominent one since it includes asymmetric couple stress tensor and there only one material length scale parameter is used in the constitutive equations. Utilising these striking features of the modified couple stress theory, a number of research works have been conducted to investigate the size-dependent behaviours of FG microbeams with various theories. The simplest one is Euler-Bernoulli beam theory or Classical Beam Theory (CBT) ([14–16]), which is applicable for thin beams only. In order to take into account the shear deformations, the Timoshenko or the First-order Beam Theory (FBT) which is appropriate for thick beams is introduced. A number of research works have been conducted to utilise this theory to study the linear responses of FG microbeams ([17–22]). The disadvantages of this theory includes the violation traction-free condition as the transverse shear stress distributes constantly through the beam's depth. Consequently, the shear correction factor which is problem-dependent needs to be considered. In order to overcome this shortcoming, Third-order Beam Theory (TBT) ([23, 24]), Sinusoidal Beam Theory (SBT) [25] and various higher-order beam theories [26, 27] are proposed. In the effort to seek a better solution for beam problems, various quasi-3D theories ([28–33]) and Carrera Unified Formulation theory ([34, 35]), which include both shear and thickness stretching effects are developed. These effects become important for very thick beams. However, as far as authors are aware, these quasi-3D theories do not use to investigate size-dependent behaviours of micro FG beams yet. These problems are interesting and need further investigation.

In this study, an unified framework for various beam theories are proposed to investigate the size-dependent bending, vibration and buckling behaviours of FG microbeams based on the modified couple stress theory. The material properties of these beams are varied through beam's depth and calculated by using classical rule of mixture and Mori-Tanaka scheme. The beam theories which are ranged from the CBT to quasi-3D are presented systematically under one unified formula. The size-dependent behaviours are then solved using the analytical Navier approach in which simply-supported boundary conditions are considered. Effects of Poisson's ratio, material length scale parameter, power-law index, estimation methods of material properties and slenderness ratio on deflections, stresses, natural frequencies and critical buckling loads of FG microbeams are examined.

The outline of this study is given as follow. The brief estimation method of material properties and constitutive equations of FGM are presented in Section 2. Section 3 shows the derivation of governing equations with respect to various beam theories. Procedure of analytical solutions which is based on Navier approach is given in Section 4. Section 5 provides a number of numerical examples in order to prove the validity and accuracy of the proposed theories for bending, vibration and buckling problems of FG microbeams. Finally, Section 6 closes the study with some concluding remarks.

2. Functionally graded materials

Consider a FG microbeam with rectangular cross-section $b \times h$ and length a, which is made of metal and ceramic. The material properties such as Young's modulus E, density ρ and Poisson's ratio ν are assumed to vary continuously through the beam's depth.

2.1. Classical rule of mixture

The effective material properties of FG microbeam are calculated by using the rule of mixture:

$$P_e = P_m V_m + P_c V_c \tag{1}$$

where P_m and P_c are the material properties of metal and ceramic, and V_m and V_c represent the volume fraction of metal and ceramic, which are assumed to be:

$$V_c(z) = (\frac{1}{2} + \frac{z}{h})^k, \quad V_m = 1 - V_c \tag{2}$$

where k is the power-law index.

2.2. Mori-Tanaka scheme

The effective bulk modulus K_e and shear modulus G_e are calculated by using Mori-Tanaka scheme [36]:

$$\frac{K_e - K_m}{K_c - K_m} = \frac{V_c}{1 + V_m \frac{K_c - K_m}{K_m + \frac{4}{3}G_m}} \tag{3a}$$

$$\frac{G_e - G_m}{G_c - G_m} = \frac{V_c}{1 + V_m \frac{G_c - G_m}{G_m + \frac{G_m(9K_m + 8G_m)}{6(K_m + 2G_m)}}} \tag{3b}$$

The effective Young's modulus E_e and Poisson's ratio ν_e are then defined as:

$$E_e = \frac{9K_e G_e}{3K_e + G_e} \tag{4a}$$

$$\nu_e = \frac{3K_e - 2G_e}{2(3K_e + G_e)} \tag{4b}$$

2.3. Constitutive Equations

The linear stress-strain relations are expressed by:

$$\left\{ \begin{array}{c} \sigma_x \\ \sigma_z \\ \sigma_{xz} \end{array} \right\} = \left[\begin{array}{ccc} \bar{C}_{11}^* & \bar{C}_{13}^* & 0 \\ \bar{C}_{13}^* & \bar{C}_{11}^* & 0 \\ 0 & 0 & C_{55} \end{array} \right] \left\{ \begin{array}{c} \epsilon_x \\ \epsilon_z \\ \gamma_{xz} \end{array} \right\} \tag{5}$$

where

$$\bar{C}_{11}^* = \bar{C}_{11} - \frac{\bar{C}_{12}^2}{\bar{C}_{22}} = \frac{E(z)}{1-\nu^2} \tag{6a}$$

$$\bar{C}_{13}^* = \bar{C}_{13} - \frac{\bar{C}_{12}\bar{C}_{23}}{\bar{C}_{22}} = \frac{E(z)\nu}{1-\nu^2} \tag{6b}$$

$$C_{55} = \frac{E(z)}{2(1+\nu)} \tag{6c}$$

For CBT, FBT and TBT, due to neglect the thickness stretching effect ($\epsilon_z = 0$), Eq. (6) is rewritten as:

$$\bar{C}_{11}^* = E(z) \tag{7a}$$

$$\bar{C}_{13}^* = 0 \tag{7b}$$

$$C_{55} = \frac{E(z)}{2(1+\nu)} \tag{7c}$$

3. Governing Equations of Motion

Based on the modified couple stress [13], the virtual strain energy can be written as:

$$\delta\mathcal{U} = \int_v (\sigma_{ij}\delta\epsilon_{ij} + m_{ij}\delta\chi_{ij})dv \quad i,j = x,y,z \tag{8}$$

where m_{ij} and χ_{ij} denote deviatoric part of the couple stress tensor, and symmetric curvature tensor, which are defined by:

$$\chi_{ij} = \frac{1}{2}(\theta_{i,j} + \theta_{j,i}) \tag{9a}$$

$$m_{ij} = \frac{E\,(z)}{1+\nu}\ell^2\chi_{ij} \tag{9b}$$

where l is a material length scale parameter and θ_i is the components of the rotation vector given by:

$$\theta_x = \theta_1 = \frac{1}{2}\left(\frac{\partial u_3}{\partial x_2} - \frac{\partial u_2}{\partial x_3}\right) \tag{10a}$$

$$\theta_y = \theta_2 = \frac{1}{2}\left(\frac{\partial u_1}{\partial x_3} - \frac{\partial u_3}{\partial x_1}\right) \tag{10b}$$

$$\theta_z = \theta_3 = \frac{1}{2}\left(\frac{\partial u_2}{\partial x_1} - \frac{\partial u_1}{\partial x_2}\right) \tag{10c}$$

The displacement fields for different beam theories can be obtained as:

$$u_1(x,z,t) = u(x,t) - z\frac{dw_b}{dx} - f(z)\frac{dw_s}{dx} \tag{11a}$$

$$u_2(x,z,t) = 0 \tag{11b}$$

$$u_3(x,z,t) = w_b(x,t) + w_s(x,t) + g(z)w_z(x,t) \tag{11c}$$

where u, w_b and w_s are the axial displacement, the bending and shear components of vertical displacement along the mid-plane of the beam. The thickness stretching effect in quasi-3D theories is taken into account by adding the component $g(z)w_z(x,t)$ in Eq. (11c). $f(z)$ and $g(z)$ are used to determine the strains and stress distribution through the beam's depth:

$$\text{CBT} : f(z) = z \tag{12a}$$

$$\text{FBT} : f(z) = 0 \tag{12b}$$

$$\text{TBT [37]} : f(z) = \frac{4z^3}{3h^2} \tag{12c}$$

$$\text{SBT [38]} : f(z) = z - \frac{h}{\pi}\sin(\frac{\pi z}{h}) \tag{12d}$$

$$\text{Quasi-3D (TBT) [37]} : f(z) = \frac{4z^3}{3h^2}; \quad g(z) = 1 - \frac{df}{dz} = 1 - \frac{4z^2}{h^2} \tag{12e}$$

$$\text{Quasi-3D (SBT) [38]} : f(z) = z - \frac{h}{\pi}\sin(\frac{\pi z}{h}); \quad g(z) = \cos(\frac{\pi z}{h}) \tag{12f}$$

The non-zero strains and symmetric curvature tensors are given by:

$$\epsilon_x = \frac{\partial u_1}{\partial x} = u' - zw_b'' - fw_s'' \tag{13a}$$

$$\gamma_{xz} = \frac{\partial u_3}{\partial x} + \frac{\partial u_1}{\partial z} = g(w_s' + w_z') \tag{13b}$$

$$\epsilon_z = \frac{\partial u_3}{\partial z} = g'w_z \tag{13c}$$

$$\chi_{xy} = \frac{1}{2}\frac{\partial \theta_y}{\partial x} = -\frac{1}{2}(w_b'' + w_s'') + \frac{g}{4}(w_s'' - w_z'') \tag{13d}$$

$$\chi_{yz} = \frac{1}{2}\frac{\partial \theta_y}{\partial z} = \frac{g'}{4}(w_s' - w_z') \tag{13e}$$

where prime ($'$) indicates the differentiation with respect to the x-axis.

3.1. Quasi-3D shear theories

Hamilton's principle is used to derive the equations of motion:

$$\delta \int_{t_1}^{t_2} (\mathcal{K} - \mathcal{U} - \mathcal{V})dt = 0 \tag{14}$$

where $\mathcal{U}, \mathcal{K}$ and $\mathcal{V}$ denote the strain energy, kinetic energy and potential energy, respectively.

The variation of the strain energy can be stated as:

$$\begin{aligned}
\delta\mathcal{U} &= \int_V (\sigma_x\delta\epsilon_x + \sigma_{xz}\delta\gamma_{xz} + \sigma_z\delta\epsilon_z + 2m_{xy}\delta\chi_{xy} + 2m_{yz}\delta\chi_{yz})dV \\
&= \int_0^l \big[N_x\delta u' - M_x^b\delta w_b'' - M_x^s\delta w_s'' + Q_{xz}(\delta w_s' + \delta w_z') + R_z\delta w_z \\
&- R_{xy}\delta(w_b'' + w_s'') + \frac{S_{xy}}{2}\delta(w_s'' - w_z'') + \frac{T_{yz}}{2}\delta(w_s' - w_z')\big]dx \qquad (15)
\end{aligned}$$

where $N_x, M_x^b, M_x^s, Q_{xz}, R_z, R_{xy}, S_{xy}$ and T_{yz} are the stress resultants, respectively, defined as:

$$N_x = \int_A \sigma_x dA = Au' - Bw_b'' - B_s w_s'' + Xw_z \qquad (16a)$$

$$M_x^b = \int_A z\sigma_x dA = Bu' - Dw_b'' - D_s w_s'' + Yw_z \qquad (16b)$$

$$M_x^s = \int_A f\sigma_x dA = B_s u' - D_s w_b'' - Hw_s'' + Y_s w_z \qquad (16c)$$

$$Q_{xz} = \int_A g\sigma_{xz} dA = A_s(w_s' + w_z') \qquad (16d)$$

$$R_z = \int_A \sigma_z g' dA = Xu' - Yw_b'' - Y_s w_s'' + Zw_z \qquad (16e)$$

$$R_{xy} = \int_A m_{xy} dA = -A_n(w_b'' + w_s'') + \frac{B_n}{2}(w_s'' - w_z'') \qquad (16f)$$

$$S_{xy} = \int_A g m_{xy} dA = -B_n(w_b'' + w_s'') + \frac{D_n}{2}(w_s'' - w_z'') \qquad (16g)$$

$$T_{yz} = \int_A g' m_{yz} dA = \frac{H_n}{2}(w_s' - w_z') \qquad (16h)$$

where

$$(A, B, B_s, D, D_s, H, Z) = \int_{-h/2}^{h/2} (1, z, f, z^2, fz, f^2, g'^2)\bar{C}_{11}^* b dz \qquad (17a)$$

$$A_s = \int_{-h/2}^{h/2} g^2 C_{55} b dz \qquad (17b)$$

$$(X, Y, Y_s) = \int_{-h/2}^{h/2} g'(1, z, f)\bar{C}_{13}^* b dz \qquad (17c)$$

$$(A_n, B_n, D_n, H_n) = \int_{-h/2}^{h/2} \left(1, g, g^2, g'^2\right) \frac{\ell^2 E(z)}{2(1+\nu)} dz \qquad (17d)$$

The variation of the potential energy by the axial force P_0 and a vertical load q is expressed by:

$$\delta\mathcal{V} = -\int_0^l \Big[P_0\big[\delta w_b'(w_b' + w_s') + \delta w_s'(w_b' + w_s')\big] + q(\delta w_b + \delta w_s)\Big]dx \qquad (18)$$

The variation of the kinetic energy is expressed by:

$$\begin{aligned}
\delta\mathcal{K} &= \int_{t_1}^{t_2}\int_V \rho\,(z)\,(\dot{u}_1\delta\dot{u}_1 + \dot{u}_2\delta\dot{u}_2 + \dot{u}_3\delta\dot{u}_3)dV dt \\
&= \int_0^l \Big[\delta\dot{u}(m_0\dot{u} - m_1\dot{w}_b{}' - m_f\dot{w}_s{}') + \delta\dot{w}_b[m_0(\dot{w}_b + \dot{w}_s) + m_g\dot{w}_z] \\
&+ \delta\dot{w}_b{}'(-m_1\dot{u} + m_2\dot{w}_b{}' + m_{fz}\dot{w}_s{}') + \delta\dot{w}_s[m_0(\dot{w}_b + \dot{w}_s) + m_g\dot{w}_z] \\
&+ \delta\dot{w}_s{}'(-m_f\dot{u} + m_{fz}\dot{w}_b{}' + m_{f^2}\dot{w}_s{}') + \delta\dot{w}_z[m_g(\dot{w}_b + \dot{w}_s) + m_{g^2}\dot{w}_z]\Big]dx
\end{aligned} \tag{19}$$

where

$$(m_0, m_1, m_2) = \int_{-h/2}^{h/2} \rho(1, z, z^2)bdz \tag{20a}$$

$$(m_f, m_{fz}, m_{f^2}) = \int_{-h/2}^{h/2} \rho(f, fz, f^2)bdz \tag{20b}$$

$$(m_g, m_{g^2}) = \int_{-h/2}^{h/2} \rho(g, g^2)bdz \tag{20c}$$

By substituting Eqs. (15), (18) and (19) into Eq. (14), the following weak statement is obtained:

$$\begin{aligned}
0 &= \int_{t_1}^{t_2}\int_0^l \Big[\delta\dot{u}(m_0\dot{u} - m_1\dot{w}_b{}' - m_f\dot{w}_s{}') + \delta\dot{w}_b[m_0(\dot{w}_b + \dot{w}_s) + m_g\dot{w}_z] + \delta\dot{w}_b{}'(-m_1\dot{u} + m_2\dot{w}_b{}' + m_{fz}\dot{w}_s{}') \\
&+ \delta\dot{w}_s[m_0(\dot{w}_b + \dot{w}_s) + m_g\dot{w}_z] + \delta\dot{w}_s{}'(-m_f\dot{u} + m_{fz}\dot{w}_b{}' + m_{f^2}\dot{w}_s{}') + \delta\dot{w}_z[m_g(\dot{w}_b + \dot{w}_s) + m_{g^2}\dot{w}_z] \\
&- N_x\delta u' + M_x^b\delta w_b'' + M_x^s\delta w_s'' - Q_{xz}\delta(w_s' + w_z') - R_z\delta w_z + R_{xy}\delta(w_b'' + w_s'') - \frac{S_{xy}}{2}\delta(w_s'' - w_z'') \\
&- \frac{T_{yz}}{2}\delta(w_s' - w_z') + P_0\big[\delta w_b'(w_b' + w_s') + \delta w_s'(w_b' + w_s')\big] + q(\delta w_b + \delta w_s)\Big]dxdt
\end{aligned} \tag{21}$$

By integrating Eq. (14) by parts and collecting the coefficients of $\delta u, \delta w_b, \delta w_s$ and δw_z, the equations of motion can be obtained:

$$N_x' = m_0\ddot{u} - m_1\ddot{w}_b{}' - m_f\ddot{w}_s{}' \tag{22a}$$

$$\begin{aligned}
M_x^{b\prime\prime} + R_{xy}'' - P_0(w_b'' + w_s'') + q &= m_1\ddot{u}' + m_0(\ddot{w}_b + \ddot{w}_s) - m_2\ddot{w}_b{}'' \\
&- m_{fz}\ddot{w}_s{}'' + m_g\ddot{w}_z
\end{aligned} \tag{22b}$$

$$\begin{aligned}
M_x^{s\prime\prime} + Q_{xz}' + R_{xy}'' - \frac{S_{xy}''}{2} - \frac{T_{yz}'}{2} - P_0(w_b'' + w_s'') + q &= m_f\ddot{u}' + m_0(\ddot{w}_b + \ddot{w}_s) - m_{fz}\ddot{w}_b{}'' \\
&- m_{f^2}\ddot{w}_s{}'' + m_g\ddot{w}_z
\end{aligned} \tag{22c}$$

$$Q_{xz}' - R_z + \frac{S_{xy}''}{2} + \frac{T_{yz}'}{2} = m_g(\ddot{w}_b + \ddot{w}_s) + m_{g^2}\ddot{w}_z \tag{22d}$$

Eq. (22) is rewritten in term of displacements by using Eq. (16):

$$Au'' - Bw_b''' - B_s w_s''' + Xw_z' = m_0\ddot{u} - m_1\ddot{w}_b{}' - m_f\ddot{w}_s{}' \quad (23a)$$

$$\begin{aligned} Bu''' - (A_n + D)w_b^{iv} - (A_n - \frac{B_n}{2} + D_s)w_s^{iv} - \frac{B_n}{2}w_z^{iv} + Yw_z'' & \\ -P_0(w_b'' + w_s'') + q &= m_1\ddot{u}' + m_0(\ddot{w}_b + \ddot{w}_s) - m_2\ddot{w}_b{}'' \\ &- m_{fz}\ddot{w}_s{}'' + m_g\ddot{w}_z \end{aligned} \quad (23b)$$

$$\begin{aligned} B_s u''' - (A_n - \frac{B_n}{2} + D_s)w_b^{iv} - (A_n - B_n + \frac{D_n}{4} + H)w_s^{iv} & \\ +(A_s + \frac{H_n}{4})w_s'' - (\frac{B_n}{2} - \frac{D_n}{4})w_z^{iv} + (A_s - \frac{H_n}{4} + Y_s)w_z'' & \\ -P_0(w_b'' + w_s'') + q &= m_f\ddot{u}' + m_0(\ddot{w}_b + \ddot{w}_s) - m_{fz}\ddot{w}_b{}'' \\ &- m_{f^2}\ddot{w}_s{}'' + m_g\ddot{w}_z \end{aligned} \quad (23c)$$

$$\begin{aligned} -Xu' - \frac{B_n}{2}w_b^{iv} + Yw_b'' - (\frac{B_n}{2} - \frac{D_n}{4})w_s^{iv} + (A_s - \frac{H_n}{4} + Y_s)w_s'' & \\ -\frac{D_n}{4}w_z^{iv} + (A_s + \frac{H_n}{4})w_z'' - Zw_z &= m_g(\ddot{w}_b + \ddot{w}_s) + m_{g^2}\ddot{w}_z \end{aligned} \quad (23d)$$

3.2. HOBT and SSBT

By neglecting the shape function $g(z)$ in Eq. (11), the following weak statement is obtained:

$$\begin{aligned} 0 &= \int_{t_1}^{t_2}\int_0^l \Big[\delta\dot{u}(m_0\dot{u} - m_1\dot{w}_b{}' - m_f\dot{w}_s{}') + \delta\dot{w}_b m_0(\dot{w}_b + \dot{w}_s) + \delta\dot{w}_b{}'(-m_1\dot{u} + m_2\dot{w}_b{}' + m_{fz}\dot{w}_s{}') \\ &+ \delta\dot{w}_s m_0(\dot{w}_b + \dot{w}_s) + \delta\dot{w}_s{}'(-m_f\dot{u} + m_{fz}\dot{w}_b{}' + m_{f^2}\dot{w}_s{}') \\ &- N_x\delta u' + M_x^b\delta w_b'' + M_x^s\delta w_s'' - Q_{xz}\delta w_s' + R_{xy}\delta(w_b'' + w_s'') - \frac{S_{xy}}{2}\delta w_s'' - \frac{T_{yz}}{2}\delta w_s' \\ &+ P_0\big[\delta w_b'(w_b' + w_s') + \delta w_s'(w_b' + w_s')\big] + q(\delta w_b + \delta w_s)\Big]dxdt \end{aligned} \quad (24)$$

where $N_x, M_x^b, M_x^s, Q_{xz}, R_{xy}, S_{xy}$ and T_{yz} are defined as:

$$N_x = \int_A \sigma_x dA = Au' - Bw_b'' - B_s w_s'' \quad (25a)$$

$$M_x^b = \int_A z\sigma_x dA = Bu' - Dw_b'' - D_s w_s'' \quad (25b)$$

$$M_x^s = \int_A f\sigma_x dA = B_s u' - D_s w_b'' - Hw_s'' \quad (25c)$$

$$Q_{xz} = \int_A g\sigma_{xz} dA = A_s w_s' \quad (25d)$$

$$R_{xy} = \int_A m_{xy} dA = -A_n(w_b'' + w_s'') + \frac{B_n}{2}w_s'' \quad (25e)$$

$$S_{xy} = \int_A g m_{xy} dA = -B_n(w_b'' + w_s'') + \frac{D_n}{2}w_s'' \quad (25f)$$

$$T_{yz} = \int_A g' m_{yz} dA = \frac{H_n}{2}w_s' \quad (25g)$$

Similarly, the equations of motion can be expressed:

$$N_x' = m_0\ddot{u} - m_1\ddot{w}_b{}' - m_f\ddot{w}_s{}' \quad (26a)$$

$$M_x^{b}{}'' + R_{xy}'' - P_0(w_b'' + w_s'') + q = m_1\ddot{u}' + m_0(\ddot{w}_b + \ddot{w}_s) - m_2\ddot{w}_b{}'' - m_{fz}\ddot{w}_s{}'' \quad (26b)$$

$$M_x^{s}{}'' + Q_{xz}' + R_{xy}'' - \frac{S_{xy}''}{2} + \frac{T_{yz}'}{2} - P_0(w_b'' + w_s'') + q = m_f\ddot{u}' + m_0(\ddot{w}_b + \ddot{w}_s) - m_{fz}\ddot{w}_b{}'' - m_{f^2}\ddot{w}_s{}'' \quad (26c)$$

Eq. (26) is rewritten in term of displacements:

$$Au'' - Bw_b''' - B_sw_s''' = m_0\ddot{u} - m_1\ddot{w}_b{}' - m_f\ddot{w}_s{}' \quad (27a)$$

$$Bu''' - (A_n + D)w_b^{iv} - (A_n - \frac{B_n}{2} + D_s)w_s^{iv} - P_0(w_b'' + w_s'') + q = m_1\ddot{u}' + m_0(\ddot{w}_b + \ddot{w}_s) - m_2\ddot{w}_b{}'' - m_{fz}\ddot{w}_s{}'' \quad (27b)$$

$$B_su''' - (A_n - \frac{B_n}{2} + D_s)w_b^{iv} - (A_n - B_n + \frac{D_n}{4} + H)w_s^{iv} + (A_s + \frac{H_n}{4})w_s'' - P_0(w_b'' + w_s'') + q = m_f\ddot{u}' + m_0(\ddot{w}_b + \ddot{w}_s) - m_{fz}\ddot{w}_b{}'' - m_{f^2}\ddot{w}_s{}'' \quad (27c)$$

3.3. FBT

By considering the shape functions $f = 0, g = 1$, the following weak statement is obtained:

$$0 = \int_{t_1}^{t_2}\int_0^l \Big[\delta\dot{u}(m_0\dot{u} - m_1\dot{w}_b{}') + \delta\dot{w}_b m_0(\dot{w}_b + \dot{w}_s) + \delta\dot{w}_b{}'(-m_1\dot{u} + m_2\dot{w}_b{}') + \delta\dot{w}_s m_0(\dot{w}_b + \dot{w}_s) - N_x\delta u' + M_x^b\delta w_b'' - Q_{xz}\delta w_s' + R_{xy}\delta w_b'' + \frac{R_{xy}}{2}\delta w_s'' + P_0\big[\delta w_b'(w_b' + w_s') + \delta w_s'(w_b' + w_s')\big] + q(\delta w_b + \delta w_s)\Big]dxdt \quad (28)$$

where N_x, M_x^b, Q_{xz} and R_{xy} are defined as:

$$N_x = \int_A \sigma_x dA = Au' - Bw_b'' \quad (29a)$$

$$M_x^b = \int_A z\sigma_x dA = Bu' - Dw_b'' \quad (29b)$$

$$Q_{xz} = \int_A g\sigma_{xz} dA = A_s w_s' \quad (29c)$$

$$R_{xy} = \int_A m_{xy} dA = -A_n w_b'' - \frac{A_n}{2}w_s'' \quad (29d)$$

Similarly, the equations of motion can be expressed:

$$N_x' = m_0\ddot{u} - m_1\ddot{w}_b{}' \quad (30a)$$

$$M_x^{b}{}'' + R_{xy}'' - P_0(w_b'' + w_s'') + q = m_0(\ddot{w}_b + \ddot{w}_s) + m_1\ddot{u}' - m_2\ddot{w}_b{}'' \quad (30b)$$

$$Q_{xz}' + \frac{R_{xy}''}{2} - P_0(w_b'' + w_s'') + q = m_0(\ddot{w}_b + \ddot{w}_s) \quad (30c)$$

Eq. (30) is rewritten in term of displacements:

$$\begin{aligned}
Au'' - Bw_b''' &= m_0\ddot{u} - m_1\ddot{w}_b{}' && \text{(31a)}\\
Bu''' - (A_n + D)w_b^{iv} - \frac{A_n}{2}w_s^{iv} - P_0(w_b'' + w_s'') + q &= m_1\ddot{u}' + m_0(\ddot{w}_b + \ddot{w}_s) - m_2\ddot{w}_b{}'' && \text{(31b)}\\
-\frac{A_n}{2}w_b^{iv} - \frac{A_n}{4}w_s^{iv} + A_s w_s'' - P_0(w_b'' + w_s'') + q &= m_0(\ddot{w}_b + \ddot{w}_s) && \text{(31c)}
\end{aligned}$$

3.4. CBT

By neglecting shear component ($w_s = 0$), the following weak statement is obtained:

$$\begin{aligned}
0 &= \int_{t_1}^{t_2}\int_0^l \Big[\delta\dot{u}(m_0\dot{u} - m_1\dot{w}_b{}') + \delta\dot{w}_b m_0\dot{w}_b + \delta\dot{w}_b{}'(-m_1\dot{u} + m_2\dot{w}_b{}')\\
&- N_x\delta u' + M_x^b\delta w_b'' + R_{xy}\delta w_b'' + P_0\delta w_b' w_b' + q\delta w_b\Big]dxdt && \text{(32)}
\end{aligned}$$

By integrating Eq. (32) by parts and collecting the coefficients of δu and δw_b, the governing equations of motion can be obtained:

$$\begin{aligned}
N_x' &= m_0\ddot{u} - m_1\ddot{w}_b{}' && \text{(33a)}\\
M_x^{b\prime\prime} + R_{xy}'' - P_0 w_b'' + q &= m_0\ddot{w}_b + m_1\ddot{u}' - m_2\ddot{w}_b{}'' && \text{(33b)}
\end{aligned}$$

where N_x, M_x^b and R_{xy} are defined as:

$$\begin{aligned}
N_x &= \int_A \sigma_x dA = Au' - Bw_b'' && \text{(34a)}\\
M_x^b &= \int_A z\sigma_x dA = Bu' - Dw_b'' && \text{(34b)}\\
R_{xy} &= \int_A m_{xy} dA = -A_n w_b'' && \text{(34c)}
\end{aligned}$$

Eq. (33) can be expressed in term of displacements:

$$\begin{aligned}
Au'' - Bw_b''' &= m_0\ddot{u} - m_1\ddot{w}_b{}' && \text{(35a)}\\
Bu''' - (A_n + D)w_b^{iv} - P_0 w_b'' + q &= m_1\ddot{u}' + m_0\ddot{w}_b - m_2\ddot{w}_b{}'' && \text{(35b)}
\end{aligned}$$

4. Analytical solutions

4.1. Quasi-3D shear theories, TBT and SBT

The size-dependent behaviours are then solved using the analytical Navier approach in which simply-supported boundary conditions are considered:

$$u(x,t) = \sum_{n=1}^{\infty} U_n \cos\alpha x\, e^{i\omega t} \quad (36a)$$

$$w_b(x,t) = \sum_{n=1}^{\infty} W_{bn} \sin\alpha x\, e^{i\omega t} \quad (36b)$$

$$w_s(x,t) = \sum_{n=1}^{\infty} W_{sn} \sin\alpha x\, e^{i\omega t} \quad (36c)$$

$$w_z(x,t) = \sum_{n=1}^{\infty} W_{zn} \sin\alpha x\, e^{i\omega t} \quad (36d)$$

where $\alpha = n\pi/L$ and U_n, W_{bn}, W_{sn} and W_{zn} are the coefficients. The transverse load q is also expanded in Fourier series for an uniform load (q_o) as:

$$q(x) = \sum_{n}^{\infty} Q_n \sin\alpha x = \sum_{n}^{\infty} \frac{4q_o}{n\pi} \sin\alpha x \quad \text{with} \quad n = 1, 3, 5, ... \quad (37)$$

By substituting Eq. (36) into Eq. (35), deflections, natural frequencies and buckling loads are calculated from the following equation:

$$\left(\begin{bmatrix} K_{11} & K_{12} & K_{13} & K_{14} \\ & K_{22} - P_0\alpha^2 & K_{23} - P_0\alpha^2 & K_{24} \\ & & K_{33} - P_0\alpha^2 & K_{34} \\ \text{sym.} & & & K_{44} \end{bmatrix} - \omega^2 \begin{bmatrix} M_{11} & M_{12} & M_{13} & 0 \\ & M_{22} & M_{23} & M_{24} \\ & & M_{33} & M_{34} \\ \text{sym.} & & & M_{44} \end{bmatrix} \right) \begin{Bmatrix} U_n \\ W_{bn} \\ W_{sn} \\ W_{zn} \end{Bmatrix} = \begin{Bmatrix} 0 \\ Q_n \\ Q_n \\ 0 \end{Bmatrix} \quad (38)$$

where

$$K_{11} = A\alpha^2; \quad K_{12} = -B\alpha^3; \quad K_{13} = -B_s\alpha^3; \quad K_{14} = -X\alpha \quad (39a)$$

$$K_{22} = (A_n + D)\alpha^4; \quad K_{23} = (A_n - \frac{B_n}{2} + D_s)\alpha^4; \quad K_{24} = \frac{B_n}{2}\alpha^4 + Y\alpha^2 \quad (39b)$$

$$K_{33} = (A_n - B_n + \frac{D_n}{4} + H)\alpha^4 + (A_s + \frac{H_n}{4})\alpha^2; \quad (39c)$$

$$K_{34} = (\frac{B_n}{2} - \frac{D_n}{4})\alpha^4 + (A_s - \frac{H_n}{4} + Y_s)\alpha^2; \quad (39d)$$

$$K_{44} = \frac{D_n}{4}\alpha^4 + (A_s + \frac{H_n}{4})\alpha^2 + Z \quad (39e)$$

$$M_{11} = m_0; \quad M_{12} = -m_1\alpha; \quad M_{13} = -m_f\alpha \quad (39f)$$

$$M_{22} = m_0 + m_2\alpha^2; \quad M_{23} = m_0 + m_{fz}\alpha^2; \quad M_{24} = m_g \quad (39g)$$

$$M_{33} = m_0 + m_{f^2}\alpha^2; \quad M_{34} = m_g; \quad M_{44} = m_{g^2} \quad (39h)$$

It should be noted that TBT and SBT's solution can be obtained by neglecting the last row and column in Eq. (38).

4.2. FBT and CBT

Similarly, deflections, natural frequencies and buckling loads are calculated from the following equation:

$$\left(\begin{bmatrix} K_{11} & K_{12} & K_{13} \\ & K_{22}-P_0\alpha^2 & K_{23}-P_0\alpha^2 \\ \text{sym.} & & K_{33}-P_0\alpha^2 \end{bmatrix} - \omega^2 \begin{bmatrix} M_{11} & M_{12} & M_{13} \\ & M_{22} & M_{23} \\ \text{sym.} & & M_{33} \end{bmatrix}\right) \begin{Bmatrix} U_n \\ W_{bn} \\ W_{sn} \end{Bmatrix} = \begin{Bmatrix} 0 \\ Q_n \\ Q_n \end{Bmatrix} \quad (40)$$

where

$$K_{11} = A\alpha^2; \quad K_{12} = -B\alpha^3; \quad K_{13} = 0; \quad K_{22} = (A_n + D)\alpha^4; \quad (41a)$$

$$K_{23} = \frac{A_n}{2}\alpha^4; \quad K_{33} = \frac{A_n}{4}\alpha^4 + A_s\alpha^2 \quad (41b)$$

$$M_{11} = m_0; \quad M_{12} = -m_1\alpha; \quad M_{22} = m_0 + m_2\alpha^2; \quad M_{23} = m_0; \quad M_{33} = m_0 \quad (41c)$$

Again, CBT's solution can be obtained by neglecting the last row and column in Eq. (40).

5. Numerical Examples

In this session, a number of numerical examples are conducted to show the validity and accuracy of the proposed approaches. Unless stated otherwise, simply-supported FG microbeams with two slenderness ratio ($a/h = 5, 10$) composed of SiC ($E_c = 427$ GPa, $\rho_c = 3100$ kg/m^3, $\nu_c = 0.17$) and Al ($E_m = 70$ GPa, $\rho_c = 2702$ kg/m^3, $\nu_c = 0.3$) are considered. The material properties are estimated by Mori-Tanaka scheme and classical rule of mixture. The material length scale parameter is assumed to be $l = 15\mu$m ([18, 19]). The shear correction factor is taken as 5/6 for FBT. The dimensionless terms are defined in this paper as:

$$\overline{u}_3 = \frac{100E_m h^3}{12q_0a^4}u_3(\frac{a}{2},0); \overline{\sigma}_x = \frac{h}{q_0a}\sigma_x(\frac{a}{2},z); \overline{\sigma}_z = \frac{h}{q_0a}\sigma_z(\frac{a}{2},z); \overline{\sigma}_{xz} = \frac{h}{q_0a}\sigma_{xz}(0,z) \quad (42a)$$

$$\overline{\omega} = \omega\frac{a^2}{h}\sqrt{\frac{\rho_m}{E_m}} \quad (42b)$$

$$\overline{P}_{cr} = P_{cr}\frac{12a^2}{h^3E_m}\sqrt{\frac{\rho_m}{E_m}} \quad (42c)$$

5.1. Verification

Since there is no published data using quasi-3D theories for FG microbeams, the verification is firstly carried out for Al/Al_2O_3 beams ($a/h = 5$) without size effect (Al: $E_m = 70\text{GPa}, \nu_m = 0.3, \rho_m = 2702\text{kg/m}^3$ and Al_2O_3: $E_c = 380\text{GPa}, \nu_c = 0.3, \rho_c = 3960\text{kg/m}^3$). The deflections, fundamental frequencies and critical buckling loads are computed and given in Table 1 along with previous results. It can be seen that the obtained results are very close with those from ([28, 29]), which demonstrates the validation of the present theory.

In order to verify further, Tables 2-4 show the deflections, fundamental frequencies of SiC/Al microbeams and critical buckling loads of Al_2O_3/SUS304 microbeams (Al_2O_3: $E_c = 390$ GPa, $\rho_c = 3960$ kg/m^3, $\nu_c = 0.3$; SUS304: $E_m = 210$ GPa, $\rho_c = 8166$ kg/m^3, $\nu_c = 0.3177$), respectively. The results are calculated with four dimensionless material length scale parameters ($h/l = 1, 2, 4, 8$) from two types of constitute relations to verify and investigate the Poisson's effect. The first one includes this effect by using elastic constants extracted from 3D model ([26, 39]) $\left(C^*_{11} = \frac{E(z)[1-\nu(z)]}{[1+\nu(z)][1-2\nu(z)]}\right.$ and $C^*_{13} = \frac{E(z)\nu(z)}{[1+\nu(z)][1-2\nu(z)]}$ for all theories $\Big)$, whereas, the second one ignores it by using those from 1D model (Eq. (6) for quasi-3D theories and Eq. (7) for others). It can be seen that the results are in excellent agreement with those from previous papers ([26, 27]) for CBT, FBT, TBT and SBT with two sets of constitute relations. As expected, the results from TBT, SBT and quasi-3D theories lie between those from CBT and FBT. Due to decrement of beam's stiffness, the inclusion of Poisson's effect leads to decrease deflections and increase natural frequencies and buckling loads. This effect increases with the increase of power-law index and decrease of material length scale parameter. Besides, due to thickess stretching effect, it is less pronounced for quasi-3D theories than others. For example, with $p = 10$, the relative difference between the deflections of two constitute relations using TBT is $5.28\%, 24.45\%, 25.90\%$, whereas, it is $1.75\%, 8.66\%, 9.21\%$ using quasi-3D (TBT) for $h/l = 1, 8$ and $l = 0$, respectively (Table 2). It is worth noting that, the exclusion of Poisson's effect provides better agreement with those from experiments [40]. Therefore, in the following examples, the numerical results are computed without this effect.

5.2. Parameter study

In this section, effects of material length scale parameter, power-law index and slenderness ratio on bending, vibration and buckling responses of FG microbeams are investigated. Tables 5-8 present the deflections and stresses of SiC/Al microbeams under uniform loads. Since the results between TBT and SBT as well as between quasi-3D (TBT) and quasi-3D (SBT) theory are nearly similar, all figures are presented for TBT and quasi-3D (TBT) only. The variation of deflection versus material length scale parameter and distribution of stresses through the depth for $p = 1$ and $p = 10$ are plotted in Figs. 1-4. It is clear that the results by classical model ($l = 0$) are always higher than those obtained by size-dependent one ($l \neq 0$). For the same power-law index, Mori-Tanaka scheme always provides higher results than classical rule of mixture does. Due to very strong size effect ($h/l = 1$), very small deflections and stresses are obtained. As the size effect decreases, deflections increase with the increase power-law index and finally approach those from classical model as $h/l = 20$ (Fig. 1). Although TBT and quasi-3D (TBT) give the same axial stress, there is slightly difference in shear stress (Fig. 3). It is due to the fact that quasi-3D theory includes the thickness stretching effect. This effect, which cannot observed in FBT and TBT, is highlighted in Fig. 4. Significant difference in these two estimation material models can be seen in stress distribution.

The fundamental frequencies and critical buckling loads of SiC/Al and Al_2O_3/SUS304 microbeams are presented in Tables 9-14. Since classical model cannot capture size effect, its results are differ significantly with those from the proposed model. It is interesting to see that for classical model, due to ignoring the thickness stretching effect, the results from FBT, TBT and SBT are slightly underestimate when comparing with those from quasi-3D theories. However, when size effect is incorporated, this tendency is different and depends on size effect. For example, when this effect is strong ($h/l = 1$), fundamental frequencies from quasi-3D theories are slightly lower than those from TBT and SBT (Tables 9 and 10). The effect of length scale parameter on the frequencies and buckling loads of micro FG beams is sketched on Figs. 5 and 6. It can be seen again that when beam's depth is very small at micron scale, this effect is significant, but become negligible as beam's depth increases.

6. Conclusions

The mechanical behaviours of the functionally graded beams based on the modified couple stress theory is fully presented in this study. While the displacement fields of beams are governed by the unified framework which covers various beam theories, the modified couple stress theory efficiently captures the size-dependent effects of the small-scale beams. The numerical examples of the bending, vibration and buckling behaviours of microbeams sufficiently prove the validity and accuracy of the proposed approach. These solutions also reveal that the increase of material length scale ratio leads to the growth in beams' stiffness. Consequently, there is a decrease in displacements, stresses as well as an increase in natural frequency and critical buckling load of microbeams.

7. Acknowledgements

The authors would like to thank Dr. Huu-Tai Thai at La Trobe University for discussion and Matlab codes. The first and second authors gratefully acknowledge research support fund from Northumbria University. The fourth author gratefully acknowledges financial support from Vietnam National Foundation for Science and Technology Development (NAFOSTED) under grant number 107.02-2015.07.

8. References

[1] L. C. Trinh, T. P. Vo, A. I. Osofero, J. Lee, Fundamental frequency analysis of functionally graded sandwich beams based on the state space approach, Composite Structuresdoi:10.1016/j.compstruct.2015.11.010.

[2] J. N. Reddy, Analysis of functionally graded plates, International Journal for Numerical Methods in Engineering 47 (1-3) (2000) 663–684. doi:10.1002/(SICI)1097-0207(20000110/30)47:1/3<663::AID-NME787>3.0.CO;2-8.

[3] J. L. Mantari, Refined and generalized hybrid type quasi-3d shear deformation theory for the bending analysis of functionally graded shells, Composites Part B: Engineering 83 (2015) 142–152. doi:10.1016/j.compositesb.2015.08.048.

[4] Y. Fu, H. Du, W. Huang, S. Zhang, M. Hu, TiNi-based thin films in MEMS applications: a review, Sensors and Actuators A: Physical 112 (23) (2004) 395–408. doi:10.1016/j.sna.2004.02.019.

[5] R. H. Baughman, C. Cui, A. A. Zakhidov, Z. Iqbal, J. N. Barisci, G. M. Spinks, G. G. Wallace, A. Mazzoldi, D. D. Rossi, A. G. Rinzler, O. Jaschinski, S. Roth, M. Kertesz, Carbon Nanotube Actuators, Science 284 (5418) (1999) 1340–1344. doi:10.1126/science.284.5418.1340.

[6] N. A. Fleck, G. M. Muller, M. F. Ashby, J. W. Hutchinson, Strain gradient plasticity: Theory and experiment, Acta Metallurgica et Materialia 42 (2) (1994) 475–487. doi:10.1016/0956-7151(94)90502-9.

[7] J. S. Stolken, A. G. Evans, A microbend test method for measuring the plasticity length scale, Acta Materialia 46 (14) (1998) 5109–5115. doi:10.1016/S1359-6454(98)00153-0.

[8] D. Lam, F. Yang, A. Chong, J. Wang, P. Tong, Experiments and theory in strain gradient elasticity, Journal of the Mechanics and Physics of Solids 51 (8) (2003) 1477 – 1508. doi:http://dx.doi.org/10.1016/S0022-5096(03)00053-X.

[9] A. C. Eringen, Nonlocal polar elastic continua, International Journal of Engineering Science 10 (1) (1972) 1–16. doi:10.1016/0020-7225(72)90070-5.

[10] N. A. Fleck, J. W. Hutchinson, A phenomenological theory for strain gradient effects in plasticity, Journal of the Mechanics and Physics of Solids 41 (12) (1993) 1825–1857. doi:10.1016/0022-5096(93)90072-N.

[11] A. Eringen, Linear theory of micropolar elasticity, Journal of Applied Mathematics and Mechanics 15 (1966) 909–923.

[12] W. Nowacki, Theory of Asymmetric Elasticity, Polish Scientific Publishers, Warsaw, 1986.

[13] F. Yang, A. C. M. Chong, D. C. C. Lam, P. Tong, Couple stress based strain gradient theory for elasticity, International Journal of Solids and Structures 39 (10) (2002) 2731–2743. doi:10.1016/S0020-7683(02)00152-X.

[14] M. Asghari, M. T. Ahmadian, M. H. Kahrobaiyan, M. Rahaeifard, On the size-dependent behavior of functionally graded micro-beams, Materials & Design 31 (5) (2010) 2324–2329. doi:10.1016/j.matdes.2009.12.006.

[15] A. Nateghi, M. Salamat-talab, J. Rezapour, B. Daneshian, Size dependent buckling analysis of functionally graded micro beams based on modified couple stress theory, Applied Mathematical Modelling 36 (10) (2012) 4971–4987. doi:10.1016/j.apm.2011.12.035.

[16] B. Akgoz, O. Civalek, Free vibration analysis of axially functionally graded tapered bernoulli-euler microbeams based on the modified couple stress theory, Composite Structures 98 (0) (2013) 314 – 322. doi:http://dx.doi.org/10.1016/j.compstruct.2012.11.020.

[17] J. N. Reddy, Microstructure-dependent couple stress theories of functionally graded beams, Journal of the Mechanics and Physics of Solids 59 (11) (2011) 2382 – 2399. doi:10.1016/j.jmps.2011.06.008.

[18] L.-L. Ke, Y.-S. Wang, Size effect on dynamic stability of functionally graded microbeams based on a modified couple stress theory, Composite Structures 93 (2) (2011) 342–350. doi:10.1016/j.compstruct.2010.09.008.

[19] M. Asghari, M. Rahaeifard, M. H. Kahrobaiyan, M. T. Ahmadian, The modified couple stress functionally graded Timoshenko beam formulation, Materials & Design 32 (3) (2011) 1435–1443. doi:10.1016/j.matdes.2010.08.046.

[20] C. M. C. Roque, D. S. Fidalgo, A. J. M. Ferreira, J. N. Reddy, A study of a microstructure-dependent composite laminated Timoshenko beam using a modified couple stress theory and a meshless method, Composite Structures 96 (2013) 532–537. doi:10.1016/j.compstruct.2012.09.011.

[21] M. Simsek, T. Kocaturk, S. D. Akbas, Static bending of a functionally graded microscale Timoshenko beam based on the modified couple stress theory, Composite Structures 95 (2013) 740–747. doi:10.1016/j.compstruct.2012.08.036.

[22] H.-T. Thai, T. P. Vo, T.-K. Nguyen, J. Lee, Size-dependent behavior of functionally graded sandwich microbeams based on the modified couple stress theory, Composite Structures 123 (2015) 337–349. doi:10.1016/j.compstruct.2014.11.065.

[23] M. Salamat-talab, A. Nateghi, J. Torabi, Static and dynamic analysis of third-order shear deformation FG micro beam based on modified couple stress theory, International Journal of Mechanical Sciences 57 (1) (2012) 63–73. doi:10.1016/j.ijmecsci.2012.02.004.

[24] B. Zhang, Y. He, D. Liu, Z. Gan, L. Shen, Size-dependent functionally graded beam model based on an improved third-order shear deformation theory, European Journal of Mechanics - A/Solids 47 (0) (2014) 211 – 230. doi:http://dx.doi.org/10.1016/j.euromechsol.2014.04.009.

[25] H.-T. Thai, T. P. Vo, A size-dependent functionally graded sinusoidal plate model based on a modified couple stress theory, Composite Structures 96 (2013) 376–383. doi:10.1016/j.compstruct.2012.09.025.

[26] M. Simsek, J. N. Reddy, Bending and vibration of functionally graded microbeams using a new higher order beam theory and the modified couple stress theory, International Journal of Engineering Science 64 (2013) 37–53. doi:10.1016/j.ijengsci.2012.12.002.

[27] M. Simsek, J. N. Reddy, A unified higher order beam theory for buckling of a functionally graded microbeam embedded in elastic medium using modified couple stress theory, Composite Structures 101 (2013) 47–58. doi:10.1016/j.compstruct.2013.01.017.

[28] T. P. Vo, H.-T. Thai, T.-K. Nguyen, F. Inam, J. Lee, A quasi-3d theory for vibration and buckling of functionally graded sandwich beams, Composite Structures 119 (2015) 1–12. doi:10.1016/j.compstruct.2014.08.006.

[29] T. P. Vo, H.-T. Thai, T.-K. Nguyen, F. Inam, J. Lee, Static behaviour of functionally graded sandwich beams using a quasi-3d theory, Composites Part B: Engineering 68 (0) (2015) 59 – 74. doi:http://dx.doi.org/10.1016/j.compositesb.2014.08.030.

[30] T.-K. Nguyen, T. P. Vo, B.-D. Nguyen, J. Lee, An analytical solution for buckling and vibration analysis of functionally graded sandwich beams using a quasi-3d shear deformation theory, Composite Structures (2015) –doi:http://dx.doi.org/10.1016/j.compstruct.2015.11.074.

[31] A. I. Osofero, T. P. Vo, T.-K. Nguyen, J. Lee, Analytical solution for vibration and buckling of functionally graded sandwich beams using various quasi-3d theories, Journal of Sandwich Structures and MaterialsarXiv:http://jsm.sagepub.com/content/early/2015/04/29/1099636215582217.full.pdf+html, doi:10.1177/1099636215582217.

[32] J. L. Mantari, J. Yarasca, A simple and accurate generalized shear deformation theory for beams, Composite Structures 134 (2015) 593 – 601. doi:http://dx.doi.org/10.1016/j.compstruct.2015.08.073.

[33] J. Yarasca, J. L. Mantari, R. A. Arciniega, Hermitelagrangian finite element formulation to study functionally graded sandwich beams, Composite Structures 140 (2016) 567 – 581. doi:http://dx.doi.org/10.1016/j.compstruct.2016.01.015.

[34] D. S. Mashat, E. Carrera, A. M. Zenkour, S. A. A. Khateeb, M. Filippi, Free vibration of {FGM} layered beams by various theories and finite elements, Composites Part B: Engineering 59 (0) (2014) 269 – 278. doi:http://dx.doi.org/10.1016/j.compositesb.2013.12.008.

[35] M. Filippi, E. Carrera, A. M. Zenkour, Static analyses of {FGM} beams by various theories and finite elements, Composites Part B: Engineering 72 (0) (2015) 1 – 9. doi:http://dx.doi.org/10.1016/j.compositesb.2014.12.004.

[36] T. Mori, K. Tanaka, Average stress in matrix and average elastic energy of materials with misfitting inclusions, Acta Metallurgica 21 (5) (1973) 571–574. doi:10.1016/0001-6160(73)90064-3.

[37] J. N. Reddy, A Simple Higher-Order Theory for Laminated Composite Plates, Journal of Applied Mechanics 51 (4) (1984) 745–752. doi:10.1115/1.3167719.

[38] M. Touratier, An efficient standard plate theory, International Journal of Engineering Science 29 (8) (1991) 901–916. doi:10.1016/0020-7225(91)90165-Y.

[39] H.-T. Thai, T. P. Vo, T. Q. Bui, T.-K. Nguyen, A quasi-3D hyperbolic shear deformation theory for functionally graded plates, Acta Mechanica (2013) 1–14doi:10.1007/s00707-013-0994-z.

[40] A. M. Dehrouyeh-Semnani, M. Nikkhah-Bahrami, A discussion on incorporating the Poisson effect in microbeam models based on modified couple stress theory, International Journal of Engineering Science 86 (2015) 20–25. doi:10.1016/j.ijengsci.2014.10.003.

Table 1: Dimensionless deflections, fundamental frequencies and critical buckling load of Al_2O_3/Al beams ($a/h = 5$)

.

Response	Theory	p					
		0	0.5	1	2	5	10
Deflection	Vo et al. [29](Quasi-3D TBT)	3.1397	-	6.1334	7.8598	9.6030	10.7572
	Present (Quasi-3D TBT)	3.1397	4.7631	6.1338	7.8606	9.6037	10.7578
	Present (Quasi-3D SBT)	3.1342	4.7559	6.1237	7.8457	9.5982	10.7513
Fundamental frequency	Vo et al. [28] (Quasi-3D TBT)	5.1618	4.4240	4.0079	3.6442	3.4133	3.2903
	Present (Quasi-3D TBT)	5.1616	4.4312	4.0238	3.6689	3.4364	3.3039
	Present (Quasi-3D SBT)	5.1665	4.8238	4.4347	4.0271	3.6723	3.4374
Buckling load $\nu_c = \nu_m = 0.23$	Vo et al. [28] (Quasi-3D TBT)	49.5901	32.5867	25.2116	19.6124	16.0842	14.4116
	Present (Quasi-3D TBT)	49.6154	32.6041	25.2248	19.6219	16.0910	14.4177
	Present (Quasi-3D SBT)	49.6378	32.6097	25.2306	19.6284	16.0833	14.4172

Table 2: Dimensionless deflection of SiC/Al microbeams under uniform load ($a/h = 10$)

h/l	Theory	Reference	With Poisson effect				Without Poisson effect			
			$p = 0.3$	1	3	10	$p = 0.3$	1	3	10
1	CBT	Present	0.0566	0.0860	0.1263	0.1699	0.0578	0.0888	0.1320	0.1791
		Ref. [26]	0.0565	0.0859	0.1262	0.1698	-	-	-	-
	FBT	Present	0.0592	0.0902	0.1331	0.1798	0.0604	0.0928	0.1384	0.1884
		Ref. [26]	0.0592	0.0902	0.1330	0.1797	-	-	-	-
	TBT	Present	0.0571	0.0868	0.1273	0.1715	0.0584	0.0895	0.1330	0.1806
		Ref. [26]	0.0571	0.0867	0.1273	0.1715	-	-	-	-
	SBT	Present	0.0571	0.0868	0.1274	0.1716	0.0584	0.0895	0.1330	0.1807
		Ref. [26]	0.0571	0.0867	0.1273	0.1716	-	-	-	-
	Quasi-3D TBT	Present	0.0579	0.0882	0.1304	0.1776	0.0584	0.0894	0.1328	0.1807
	Quasi-3D SBT	Present	0.0579	0.0884	0.1309	0.1787	0.0584	0.0894	0.1328	0.1809
2	CBT	Present	0.1496	0.2228	0.3069	0.3939	0.1587	0.2426	0.3431	0.4473
		Ref. [26]	0.1496	0.2227	0.3068	0.3939	-	-	-	-
	FBT	Present	0.1538	0.2293	0.3176	0.4095	0.1627	0.2488	0.3530	0.4618
		Ref. [26]	0.1537	0.2292	0.3175	0.4095	-	-	-	-
	TBT	Present	0.1519	0.2261	0.3121	0.4017	0.1608	0.2457	0.3478	0.4543
		Ref. [26]	0.1518	0.2261	0.3121	0.4017	-	-	-	-
	SBT	Present	0.1519	0.2261	0.3123	0.4020	0.1608	0.2457	0.3479	0.4545
		Ref. [26]	0.1518	0.2261	0.3123	0.4019	-	-	-	-
	Quasi-3D TBT	Present	0.1565	0.2347	0.3291	0.4333	0.1603	0.2437	0.3447	0.4530
	Quasi-3D SBT	Present	0.1569	0.2357	0.3318	0.4387	0.1603	0.2437	0.3450	0.4535
4	CBT	Present	0.2543	0.3698	0.4777	0.5876	0.2817	0.4280	0.5715	0.7150
		Ref. [26]	0.2542	0.3698	0.4776	0.5876	-	-	-	-
	FBT	Present	0.2604	0.3794	0.4929	0.6093	0.2877	0.4372	0.5861	0.7359
		Ref. [26]	0.2603	0.3794	0.4928	0.6093	-	-	-	-
	TBT	Present	0.2594	0.3781	0.4914	0.6067	0.2866	0.4358	0.5844	0.7330
		Ref. [26]	0.2593	0.3780	0.4913	0.6067	-	-	-	-
	SBT	Present	0.2594	0.3781	0.4916	0.6069	0.2866	0.4359	0.5846	0.7332
		Ref. [26]	0.2593	0.3781	0.4916	0.6069	-	-	-	-
	Quasi-3D TBT	Present	0.2726	0.4014	0.5322	0.6777	0.2845	0.4287	0.5745	0.7275
	Quasi-3D SBT	Present	0.2737	0.4042	0.5390	0.6904	0.2845	0.4287	0.5751	0.7284
8	CBT	Present	0.3082	0.4429	0.5548	0.6700	0.3494	0.5291	0.6856	0.8408
		Ref. [26]	0.3081	0.4429	0.5548	0.6700	-	-	-	-
	FBT	Present	0.3155	0.4543	0.5724	0.6946	0.3566	0.5402	0.7029	0.8651
		Ref. [26]	0.3154	0.4542	0.5723	0.6946	-	-	-	-
	TBT	Present	0.3152	0.4545	0.5744	0.6962	0.3563	0.5404	0.7046	0.8664
		Ref. [26]	0.3150	0.4545	0.5743	0.6962	-	-	-	-
	SBT	Present	0.3152	0.4546	0.5746	0.6963	0.3563	0.5404	0.7048	0.8665
		Ref. [26]	0.3150	0.4545	0.5745	0.6963	-	-	-	-
	Quasi-3D TBT	Present	0.3346	0.4882	0.6297	0.7894	0.3529	0.5291	0.6897	0.8578
	Quasi-3D SBT	Present	0.3363	0.4923	0.6389	0.8062	0.3528	0.5292	0.6904	0.8587
Classical	CBT	Present	0.3316	0.4742	0.5864	0.7028	0.3796	0.5739	0.7341	0.8929
($l = 0$)		Ref. [26]	0.3315	0.4741	0.5864	0.7028	-	-	-	-
	FBT	Present	0.3394	0.4863	0.6050	0.7286	0.3875	0.5860	0.7527	0.9187
		Ref. [26]	0.3393	0.4862	0.6049	0.7286	-	-	-	-
	TBT	Present	0.3395	0.4874	0.6088	0.7324	0.3875	0.5871	0.7563	0.9221
		Ref. [26]	0.3394	0.4874	0.6087	0.7324	-	-	-	-
	SBT	Present	0.3395	0.4874	0.6089	0.7323	0.3875	0.5871	0.7564	0.9220
		Ref. [26]	0.3394	0.4874	0.6089	0.7323	-	-	-	-
	Quasi-3D TBT	Present	0.3619	0.5258	0.6704	0.8350	0.3833	0.5736	0.7389	0.9119
	Quasi-3D SBT	Present	0.3638	0.5305	0.6807	0.8537	0.3833	0.5737	0.7395	0.9129

Table 3: Dimensionless fundamental frequencies of SiC/Al microbeams ($a/h = 10$)

h/l	Theory	Reference	With Poisson effect				Without Poisson effect			
			$p = 0.3$	1	3	10	$p = 0.3$	1	3	10
1	CBT	Present	12.9001	10.6483	8.9420	7.8015	12.7586	10.4765	8.7436	7.5970
		Ref. [26]	12.9004	10.6483	8.9420	7.8011	-	-	-	-
	FBT	Present	12.6055	10.3983	8.7111	7.5840	12.4821	10.2486	8.5396	7.4084
		Ref. [26]	12.6058	10.3982	8.7110	7.5835	-	-	-	-
	TBT	Present	12.8333	10.6010	8.9049	7.7644	12.6967	10.4344	8.7121	7.5663
		Ref. [26]	12.8337	10.6009	8.9048	7.7640	-	-	-	-
	SBT	Present	12.8394	10.6099	8.9109	7.7649	12.6974	10.4340	8.7110	7.5647
		Ref. [26]	12.8344	10.6004	8.9034	7.7620	-	-	-	-
	Quasi-3D TBT	Present	12.7422	10.5093	8.7936	7.6236	12.6894	10.4388	8.7161	7.5587
	Quasi-3D SBT	Present	12.7371	10.5001	8.7775	7.6019	12.6906	10.4383	8.7140	7.5559
2	CBT	Present	7.9303	6.6160	5.7362	5.1234	7.6991	6.3380	5.4239	4.8071
		Ref. [26]	7.9307	6.6159	5.7362	5.1231	-	-	-	-
	FBT	Present	7.8229	6.5211	5.6383	5.0240	7.6052	6.2598	5.3470	4.7308
		Ref. [26]	7.8233	6.5211	5.6383	5.0237	-	-	-	-
	TBT	Present	7.8718	6.5671	5.6877	5.0734	7.6486	6.2988	5.3872	4.7702
		Ref. [26]	7.8722	6.5670	5.6876	5.0731	-	-	-	-
	SBT	Present	7.8811	6.5838	5.7017	5.0768	7.6489	6.2985	5.3862	4.7690
		Ref. [26]	7.8725	6.5666	5.6861	5.0713	-	-	-	-
	Quasi-3D TBT	Present	7.7504	6.4429	5.5363	4.8816	7.6582	6.3231	5.4091	4.7749
	Quasi-3D SBT	Present	7.7418	6.4294	5.5137	4.8513	7.6590	6.3227	5.4072	4.7724
4	CBT	Present	6.0835	5.1348	4.5978	4.1947	5.7793	4.7722	4.2025	3.8022
		Ref. [26]	6.0840	5.1348	4.5978	4.1945	-	-	-	-
	FBT	Present	6.0110	5.0692	4.5257	4.1186	5.7188	4.7214	4.1494	3.7474
		Ref. [26]	6.0115	5.0692	4.5256	4.1184	-	-	-	-
	TBT	Present	6.0231	5.0784	4.5327	4.1278	5.7292	4.7292	4.1556	3.7550
		Ref. [26]	6.0236	5.0783	4.5327	4.1276	-	-	-	-
	SBT	Present	6.0354	5.1025	4.5559	4.1349	5.7293	4.7290	4.1548	3.7544
		Ref. [26]	6.0237	5.0780	4.5316	4.1267	-	-	-	-
	Quasi-3D TBT	Present	5.8726	4.9262	4.3533	3.9029	5.7486	4.7672	4.1898	3.7676
	Quasi-3D SBT	Present	5.8612	4.9093	4.3262	3.8672	5.7494	4.7669	4.1881	3.7655
8	CBT	Present	5.5262	4.6920	4.2660	3.9284	5.1895	4.2923	3.8368	3.5063
		Ref. [26]	5.5267	4.6920	4.2659	3.9282	-	-	-	-
	FBT	Present	5.4612	4.6328	4.1996	3.8575	5.1361	4.2474	3.7889	3.4562
		Ref. [26]	5.4617	4.6327	4.1995	3.8573	-	-	-	-
	TBT	Present	5.4640	4.6314	4.1922	3.8531	5.1385	4.2468	3.7842	3.4537
		Ref. [26]	5.4646	4.6313	4.1922	3.8528	-	-	-	-
	SBT	Present	5.4776	4.6591	4.2201	3.8622	5.1386	4.2466	3.7838	3.4536
		Ref. [26]	5.4645	4.6311	4.1915	3.8526	-	-	-	-
	Quasi-3D TBT	Present	5.3001	4.4671	4.0022	3.6163	5.1619	4.2908	3.8238	3.4696
	Quasi-3D SBT	Present	5.2875	4.4487	3.9734	3.5785	5.1627	4.2906	3.8223	3.4678
Classical	CBT	Present	5.3275	4.5348	4.1495	3.8355	4.9788	4.1211	3.7078	3.4026
($l = 0$)		Ref. [26]	5.3280	4.5348	4.1494	3.8353	-	-	-	-
	FBT	Present	5.2648	4.4776	4.0849	3.7663	4.9276	4.0780	3.6615	3.3540
		Ref. [26]	5.2654	4.4775	4.0848	3.7661	-	-	-	-
	TBT	Present	5.2644	4.4724	4.0720	3.7566	4.9273	4.0744	3.6527	3.3477
		Ref. [26]	5.2649	4.4723	4.0719	3.7564	-	-	-	-
	SBT	Present	5.2786	4.5016	4.1019	3.7666	4.9273	4.0743	3.6524	3.3478
		Ref. [26]	5.2650	4.4722	4.0715	3.7565	-	-	-	-
	Quasi-3D TBT	Present	5.0964	4.3042	3.8787	3.5160	4.9523	4.1209	3.6944	3.3649
	Quasi-3D SBT	Present	5.0832	4.2852	3.8493	3.4775	4.9531	4.1207	3.6930	3.3633

Table 4: Dimensionless critical buckling loads of Al_2O_3/SUS304 microbeams ($a/h = 10$)

h/l	Theory	Reference	With Poisson effect				Without Poisson effect			
			$p=0$	0.5	1	10	$p=0$	0.5	1	10
1	CBT	Present	109.2706	88.8923	80.9467	63.6997	102.9259	83.5272	75.8559	59.1987
		Ref. [27]	-	-	-	-	102.9258	83.5292	75.8558	59.1987
	FBT	Present	107.7255	90.5034	82.4063	63.5569	101.6569	82.5099	74.9253	58.4445
		Ref. [27]	-	-	-	-	101.7143	82.5580	74.9674	58.4786
	TBT	Present	108.9131	91.4867	83.3159	64.3237	102.6399	83.2946	75.6501	59.0435
		Ref. [27]	-	-	-	-	102.6398	83.2967	75.6500	59.0434
	SBT	Present	108.9158	91.4901	83.3179	64.3218	102.6425	83.2973	75.6516	59.0425
		Ref. [27]	-	-	-	-	102.6425	83.2994	75.6516	59.0424
	Quasi-3D TBT	Present	104.4661	87.6181	79.7097	61.0582	102.6622	86.0353	78.2045	59.7993
	Quasi-3D SBT	Present	104.1111	87.3333	79.4222	60.7151	102.6911	86.0600	78.2260	59.8125
2	CBT	Present	45.8232	37.1353	34.0872	27.7156	39.4784	31.7701	28.9964	23.2146
		Ref. [27]	-	-	-	-	39.4784	31.7713	28.9963	23.2146
	FBT	Present	45.3928	37.9704	34.7503	27.8442	39.1884	31.5421	28.7854	23.0333
		Ref. [27]	-	-	-	-	39.2016	31.5537	28.7950	23.0415
	TBT	Present	45.5832	38.1262	34.8962	27.9781	39.3205	31.6455	28.8823	23.1189
		Ref. [27]	-	-	-	-	39.3205	31.6467	28.8823	23.1188
	SBT	Present	45.5840	38.1273	34.8968	27.9770	39.3213	31.6463	28.8828	23.1185
		Ref. [27]	-	-	-	-	39.3213	31.6475	28.8276	23.1184
	Quasi-3D TBT	Present	41.1488	34.2661	31.2999	24.7285	39.3449	32.6832	29.7946	23.4698
	Quasi-3D SBT	Present	40.7918	33.9789	31.0108	24.3864	39.3719	32.7058	29.8147	23.4835
4	CBT	Present	29.9613	24.1960	22.3724	18.7196	23.6166	18.8309	17.2815	14.2186
		Ref. [27]	-	-	-	-	23.6165	18.8318	17.2815	14.2185
	FBT	Present	29.7025	24.7468	22.7544	18.8547	23.4637	18.7124	17.1709	14.1195
		Ref. [27]	-	-	-	-	23.4706	18.7187	17.1759	14.1239
	TBT	Present	29.7443	24.7818	22.7864	18.8821	23.4897	18.7328	17.1896	14.1356
		Ref. [27]	-	-	-	-	23.4896	18.7337	17.1895	14.1355
	SBT	Present	29.7447	24.7822	22.7867	18.8817	23.4900	18.7331	17.1897	14.1355
		Ref. [27]	-	-	-	-	23.4900	18.7340	17.1897	14.1354
	Quasi-3D TBT	Present	25.3195	20.9280	19.1974	15.6454	23.5156	19.3452	17.6922	14.3868
	Quasi-3D SBT	Present	24.9619	20.6401	18.9079	15.3040	23.5421	19.3672	17.7119	14.4008
8	CBT	Present	25.9958	20.9612	19.4436	16.4706	19.6511	15.5960	14.3528	11.9696
		Ref. [27]	-	-	-	-	19.6510	15.5969	14.3528	11.9695
	FBT	Present	25.7731	21.4352	19.7502	16.6035	19.5257	15.4994	14.2623	11.8872
		Ref. [27]	-	-	-	-	19.5314	15.5047	14.2664	11.8909
	TBT	Present	25.7833	21.4448	19.7579	16.6058	19.5318	15.5045	14.2662	11.8892
		Ref. [27]	-	-	-	-	19.5317	15.5053	14.2661	11.8892
	SBT	Present	25.7836	21.4451	19.7582	16.6059	19.5320	15.5046	14.2663	11.8893
		Ref. [27]	-	-	-	-	19.5319	15.5055	14.2662	11.8892
	Quasi-3D TBT	Present	21.3621	17.5935	16.1718	13.3745	19.5583	16.0106	14.6665	12.1160
	Quasi-3D SBT	Present	21.0045	17.3053	15.8822	13.0333	19.5847	16.0325	14.6862	12.1300
Classical ($l=0$)	CBT	Present	24.6825	19.8898	18.4736	15.7257	18.3293	14.5178	13.3766	11.2199
		Ref. [27]	-	-	-	-	18.3292	14.5186	13.3765	11.2198
	FBT	Present	24.4711	20.3379	18.7548	15.8575	18.2208	14.4348	13.2985	11.1475
		Ref. [27]	-	-	-	-	18.2177	14.4329	13.2961	11.1462
	TBT	Present	24.4712	20.3395	18.7547	15.8516	18.2209	14.4352	13.2979	11.1452
		Ref. [27]	-	-	-	-	18.2124	14.4292	13.2916	11.1403
	SBT	Present	24.4715	20.3397	18.7550	15.8518	18.2211	14.4354	13.2980	11.1453
		Ref. [27]	-	-	-	-	18.2126	14.4293	13.2917	11.1405
	Quasi-3D TBT	Present	20.0515	16.4891	15.1697	12.6223	18.2476	14.9062	13.6645	11.3638
	Quasi-3D SBT	Present	19.6937	16.2009	14.8801	12.2813	18.2739	14.9281	13.6841	11.3779

Table 5: Dimensionless deflections of SiC/Al microbeams under uniform load ($a/h = 5$)

h/l	Theory	Mori-Tanaka scheme				Classical rule of mixture			
		$p = 0$	0.5	1	10	$p = 0$	0.5	1	10
1	CBT	0.0348	0.0685	0.0888	0.1791	0.0348	0.0504	0.0638	0.1512
	FBT	0.0412	0.0806	0.1047	0.2156	0.0412	0.0594	0.0748	0.1816
	TBT	0.0363	0.0710	0.0917	0.1849	0.0363	0.0525	0.0662	0.1555
	SBT	0.0362	0.0710	0.0917	0.1852	0.0362	0.0525	0.0661	0.1557
	Quasi-3D TBT	0.0364	0.0712	0.0920	0.1865	0.0364	0.0527	0.0663	0.1565
	Quasi-3D SBT	0.0364	0.0713	0.0920	0.1870	0.0364	0.0527	0.0663	0.1569
2	CBT	0.0935	0.1886	0.2426	0.4473	0.0935	0.1390	0.1781	0.3804
	FBT	0.1034	0.2070	0.2669	0.5048	0.1034	0.1525	0.1948	0.4283
	TBT	0.0988	0.1982	0.2547	0.4748	0.0988	0.1464	0.1870	0.4026
	SBT	0.0988	0.1981	0.2548	0.4757	0.0988	0.1463	0.1869	0.4035
	Quasi-3D TBT	0.0990	0.1975	0.2534	0.4759	0.0990	0.1461	0.1861	0.4021
	Quasi-3D SBT	0.0989	0.1975	0.2535	0.4771	0.0989	0.1461	0.1861	0.4034
4	CBT	0.1616	0.3356	0.4280	0.7150	0.1616	0.2475	0.3229	0.6127
	FBT	0.1764	0.3636	0.4647	0.7983	0.1764	0.2681	0.3485	0.6823
	TBT	0.1738	0.3588	0.4590	0.7864	0.1738	0.2644	0.3439	0.6753
	SBT	0.1737	0.3588	0.4591	0.7873	0.1737	0.2643	0.3439	0.6766
	Quasi-3D TBT	0.1734	0.3546	0.4516	0.7809	0.1734	0.2623	0.3391	0.6670
	Quasi-3D SBT	0.1734	0.3546	0.4518	0.7822	0.1734	0.2622	0.3391	0.6689
8	CBT	0.1976	0.4169	0.5291	0.8408	0.1976	0.3076	0.4053	0.7231
	FBT	0.2154	0.4511	0.5737	0.9380	0.2154	0.3328	0.4367	0.8045
	TBT	0.2145	0.4501	0.5743	0.9428	0.2145	0.3312	0.4353	0.8161
	SBT	0.2144	0.4501	0.5744	0.9430	0.2144	0.3312	0.4352	0.8170
	Quasi-3D TBT	0.2136	0.4426	0.5615	0.9313	0.2136	0.3274	0.4269	0.8010
	Quasi-3D SBT	0.2136	0.4426	0.5617	0.9322	0.2136	0.3274	0.4269	0.8026
Classical	CBT	0.2133	0.4532	0.5739	0.8929	0.2133	0.3345	0.4427	0.7690
($l = 0$)	FBT	0.2325	0.4904	0.6223	0.9961	0.2325	0.3619	0.4770	0.8556
	TBT	0.2325	0.4915	0.6264	1.0097	0.2325	0.3615	0.4772	0.8773
	SBT	0.2325	0.4915	0.6265	1.0094	0.2325	0.3614	0.4772	0.8778
	Quasi-3D TBT	0.2314	0.4822	0.6108	0.9950	0.2314	0.3568	0.4669	0.8585
	Quasi-3D SBT	0.2313	0.4823	0.6109	0.9956	0.2313	0.3567	0.4670	0.8599

Table 6: Dimensionless deflections of SiC/Al microbeams under uniform load ($a/h = 10$)

h/l	Theory	Mori-Tanaka scheme				Classical rule of mixture			
		$p = 0$	0.5	1	10	$p = 0$	0.5	1	10
1	CBT	0.0348	0.0685	0.0888	0.1791	0.0348	0.0504	0.0638	0.1512
	FBT	0.0364	0.0716	0.0928	0.1884	0.0364	0.0527	0.0666	0.1589
	TBT	0.0352	0.0691	0.0895	0.1806	0.0352	0.0510	0.0644	0.1523
	SBT	0.0352	0.0691	0.0895	0.1807	0.0352	0.0510	0.0644	0.1523
	Quasi-3D TBT	0.0352	0.0691	0.0894	0.1807	0.0352	0.0510	0.0643	0.1521
	Quasi-3D SBT	0.0352	0.0691	0.0894	0.1809	0.0352	0.0510	0.0643	0.1522
2	CBT	0.0935	0.1886	0.2426	0.4473	0.0935	0.1390	0.1781	0.3804
	FBT	0.0960	0.1932	0.2488	0.4618	0.0960	0.1424	0.1823	0.3925
	TBT	0.0949	0.1910	0.2457	0.4543	0.0949	0.1408	0.1804	0.3860
	SBT	0.0949	0.1910	0.2457	0.4545	0.0949	0.1408	0.1803	0.3863
	Quasi-3D TBT	0.0949	0.1900	0.2437	0.4530	0.0949	0.1404	0.1792	0.3833
	Quasi-3D SBT	0.0949	0.1900	0.2437	0.4535	0.0949	0.1404	0.1792	0.3838
4	CBT	0.1616	0.3356	0.4280	0.7150	0.1616	0.2475	0.3229	0.6127
	FBT	0.1653	0.3426	0.4372	0.7359	0.1653	0.2527	0.3293	0.6302
	TBT	0.1647	0.3414	0.4358	0.7330	0.1647	0.2518	0.3282	0.6285
	SBT	0.1647	0.3414	0.4359	0.7332	0.1647	0.2517	0.3282	0.6288
	Quasi-3D TBT	0.1646	0.3376	0.4287	0.7275	0.1646	0.2502	0.3239	0.6196
	Quasi-3D SBT	0.1646	0.3376	0.4287	0.7284	0.1646	0.2501	0.3239	0.6206
8	CBT	0.1976	0.4169	0.5291	0.8408	0.1976	0.3076	0.4053	0.7231
	FBT	0.2021	0.4254	0.5402	0.8651	0.2021	0.3139	0.4132	0.7435
	TBT	0.2018	0.4252	0.5404	0.8664	0.2018	0.3135	0.4128	0.7464
	SBT	0.2018	0.4252	0.5404	0.8665	0.2018	0.3135	0.4128	0.7467
	Quasi-3D TBT	0.2016	0.4190	0.5291	0.8578	0.2016	0.3109	0.4058	0.7332
	Quasi-3D SBT	0.2016	0.4190	0.5292	0.8587	0.2016	0.3108	0.4058	0.7343
Classical	CBT	0.2133	0.4532	0.5739	0.8929	0.2133	0.3345	0.4427	0.7690
($l = 0$)	FBT	0.2181	0.4625	0.5860	0.9187	0.2181	0.3413	0.4513	0.7906
	TBT	0.2181	0.4628	0.5871	0.9221	0.2181	0.3412	0.4513	0.7961
	SBT	0.2181	0.4628	0.5871	0.9220	0.2181	0.3412	0.4513	0.7962
	Quasi-3D TBT	0.2179	0.4554	0.5736	0.9119	0.2179	0.3381	0.4429	0.7807
	Quasi-3D SBT	0.2178	0.4554	0.5737	0.9129	0.2178	0.3380	0.4429	0.7818

Table 7: Dimensionless axial stress $\sigma_x(a/2, h/2)$ of SiC/Al microbeams under uniform load $(a/h = 5)$

h/l	Theory	Mori-Tanaka scheme				Classical rule of mixture			
		$p = 0$	0.5	1	10	$p = 0$	0.5	1	10
1	CBT	0.6119	0.9204	1.1128	2.6143	0.6119	0.7493	0.8520	1.9549
	FBT	0.5436	0.8187	0.9895	2.3130	0.5436	0.6665	0.7584	1.7304
	TBT	0.5987	0.9039	1.0941	2.5638	0.5987	0.7345	0.8367	1.9205
	SBT	0.5990	0.9043	1.0942	2.5613	0.5990	0.7351	0.8372	1.9185
	Quasi-3D TBT	0.6001	0.9082	1.1014	2.5431	0.6001	0.7367	0.8422	1.9205
	Quasi-3D SBT	0.6031	0.9145	1.1092	2.5593	0.6031	0.7417	0.8481	1.9326
2	CBT	1.6433	2.5336	3.0407	6.5295	1.6433	2.0639	2.3801	4.9192
	FBT	1.5865	2.4475	2.9369	6.2943	1.5865	1.9938	2.3001	4.7428
	TBT	1.6245	2.5114	3.0142	6.4505	1.6245	2.0448	2.3601	4.8630
	SBT	1.6255	2.5130	3.0158	6.4506	1.6255	2.0463	2.3618	4.8625
	Quasi-3D TBT	1.6284	2.5137	3.0187	6.3948	1.6284	2.0447	2.3634	4.8485
	Quasi-3D SBT	1.6365	2.5314	3.0408	6.4414	1.6284	2.0447	2.3634	4.8485
4	CBT	2.8398	4.5094	5.3636	10.4371	2.8398	3.6764	4.3150	7.9226
	FBT	2.8099	4.4623	5.3075	10.3243	2.8099	3.6381	4.2702	7.8372
	TBT	2.8450	4.5277	5.3876	10.4667	2.8450	3.6891	4.3319	7.9555
	SBT	2.8470	4.5315	5.3925	10.4753	2.8470	3.6919	4.3354	7.9630
	Quasi-3D TBT	2.8479	4.5034	5.3519	10.3383	2.8479	3.6718	4.3053	7.8851
	Quasi-3D SBT	2.8620	4.5354	5.3920	10.4199	2.8620	3.6970	4.3367	7.9491
8	CBT	3.4718	5.6014	6.6299	12.2733	3.4718	4.5689	5.4156	9.3497
	FBT	3.4618	5.5853	6.6108	12.2376	3.4618	4.5557	5.4000	9.3225
	TBT	3.5037	5.6662	6.7142	12.4263	3.5037	4.6164	5.4752	9.4918
	SBT	3.5064	5.6714	6.7211	12.4384	3.5064	4.6202	5.4800	9.5034
	Quasi-3D TBT	3.5036	5.6138	6.6361	12.2402	3.5036	4.5821	5.4167	9.3708
	Quasi-3D SBT	3.5208	5.6540	6.6860	12.3379	3.5208	4.6135	5.4565	9.4487
Classical	CBT	3.7500	6.0933	7.1962	13.0379	3.7500	4.9711	5.9188	9.9470
$(l = 0)$	FBT	3.7500	6.0933	7.1962	13.0379	3.7500	4.9711	5.9188	9.9470
	TBT	3.7968	6.1847	7.3155	13.2591	3.7968	5.0383	6.0031	10.1515
	SBT	3.7998	6.1906	7.3234	13.2719	3.7998	5.0427	6.0086	10.1642
	Quasi-3D TBT	3.7947	6.1164	7.2134	13.0431	3.7947	4.9945	5.9263	10.0034
	Quasi-3D SBT	3.8133	6.1602	7.2677	13.1470	3.8133	5.0287	5.9701	10.0866

Table 8: Dimensionless shear stress $\sigma_{xz}(0,0)$ of SiC/Al microbeams under uniform load ($a/h = 5$)

h/l	Theory	Mori-Tanaka scheme				Classical rule of mixture			
		$p = 0$	0.5	1	10	$p = 0$	0.5	1	10
1	FBT	0.3181	0.2948	0.2612	0.2583	0.3181	0.3296	0.3104	0.2173
	TBT	0.1019	0.0896	0.0727	0.0656	0.1019	0.1091	0.0977	0.0506
	SBT	0.1049	0.0929	0.0766	0.0719	0.1049	0.1114	0.1007	0.0559
	Quasi-3D TBT	0.1064	0.0959	0.0798	0.0773	0.1064	0.1146	0.1036	0.0602
	Quasi-3D SBT	0.1095	0.0995	0.0840	0.0840	0.1095	0.1173	0.1069	0.0660
2	FBT	0.4002	0.3683	0.3271	0.3303	0.4002	0.4118	0.3862	0.2774
	TBT	0.2868	0.2600	0.2258	0.2225	0.2868	0.2972	0.2744	0.1842
	SBT	0.2955	0.2693	0.2365	0.2386	0.2955	0.3047	0.2829	0.1996
	Quasi-3D TBT	0.2926	0.2698	0.2370	0.2393	0.2926	0.3057	0.2840	0.1990
	Quasi-3D SBT	0.3014	0.2793	0.2479	0.2555	0.2926	0.3057	0.2840	0.1990
4	FBT	0.5020	0.4641	0.4116	0.4085	0.5020	0.5190	0.4878	0.3436
	TBT	0.5242	0.4922	0.4500	0.4584	0.5242	0.5361	0.5098	0.4066
	SBT	0.5402	0.5088	0.4681	0.4808	0.5402	0.5512	0.5256	0.4304
	Quasi-3D TBT	0.5240	0.4959	0.4552	0.4664	0.5240	0.5383	0.5136	0.4143
	Quasi-3D SBT	0.5398	0.5123	0.4731	0.4881	0.5398	0.5534	0.5293	0.4377
8	FBT	0.5625	0.5231	0.4631	0.4508	0.5625	0.5850	0.5519	0.3798
	TBT	0.6643	0.6357	0.5932	0.6060	0.6643	0.6790	0.6553	0.5562
	SBT	0.6845	0.6564	0.6151	0.6286	0.6845	0.6988	0.6755	0.5815
	Quasi-3D TBT	0.6582	0.6317	0.5906	0.6045	0.6582	0.6737	0.6513	0.5553
	Quasi-3D SBT	0.6779	0.6520	0.6120	0.6262	0.6779	0.6931	0.6710	0.5798
Classical	FBT	0.5976	0.5576	0.4931	0.4752	0.5976	0.6237	0.5896	0.4006
($l = 0$)	TBT	0.7341	0.7084	0.6667	0.6802	0.7341	0.7508	0.7295	0.6343
	SBT	0.7558	0.7309	0.6899	0.7019	0.7558	0.7725	0.7514	0.6591
	Quasi-3D TBT	0.7240	0.6993	0.6589	0.6730	0.7240	0.7403	0.7199	0.6281
	Quasi-3D SBT	0.7451	0.7211	0.6814	0.6936	0.7451	0.7613	0.7412	0.6521

Table 9: Dimensionless fundamental frequencies of SiC/Al microbeams ($a/h = 5$)

h/l	Theory	Mori-Tanaka scheme				Classical rule of mixture			
		$p = 0$	0.5	1	10	$p = 0$	0.5	1	10
1	CBT	16.0020	11.6321	10.3181	7.4958	16.0020	13.5770	12.1927	8.1401
	FBT	14.7917	10.7926	9.5724	6.8775	14.7917	12.5885	11.3293	7.4837
	TBT	15.7140	11.4489	10.1757	7.3899	15.7140	13.3318	11.9948	8.0425
	SBT	15.7174	11.4501	10.1748	7.3849	15.7174	13.3364	11.9971	8.0375
	Quasi-3D TBT	15.6249	11.3964	10.1345	7.3354	15.6249	13.2627	11.9444	7.9967
	Quasi-3D SBT	15.6304	11.3984	10.1336	7.3285	15.6304	13.2692	11.9477	7.9887
2	CBT	9.7649	7.0135	6.2452	4.7439	9.7649	8.1817	7.2974	5.1338
	FBT	9.3153	6.7150	5.9757	4.4815	9.3153	7.8316	6.9992	4.8579
	TBT	9.5175	6.8550	6.1087	4.6144	9.5175	7.9867	7.1369	5.0026
	SBT	9.5191	6.8554	6.1078	4.6104	9.5191	7.9888	7.1380	4.9975
	Quasi-3D TBT	9.4917	6.8550	6.1160	4.5998	9.4917	7.9776	7.1420	4.9979
	Quasi-3D SBT	9.4950	6.8561	6.1154	4.5952	9.4950	7.9809	7.1435	4.9913
4	CBT	7.4281	5.2575	4.7027	3.7523	7.4281	6.1304	5.4202	4.0457
	FBT	7.1237	5.0613	4.5236	3.5599	7.1237	5.9008	5.2281	3.8445
	TBT	7.1753	5.0937	4.5509	3.5864	7.1753	5.9407	5.2614	3.8645
	SBT	7.1761	5.0938	4.5503	3.5846	7.1761	5.9416	5.2619	3.8610
	Quasi-3D TBT	7.1713	5.1170	4.5826	3.5927	7.1713	5.9547	5.2913	3.8833
	Quasi-3D SBT	7.1738	5.1179	4.5823	3.5902	7.1738	5.9568	5.2922	3.8786
8	CBT	6.7181	4.7173	4.2300	3.4603	6.7181	5.4993	4.8382	3.7243
	FBT	6.4448	4.5428	4.0701	3.2832	6.4448	5.2952	4.6687	3.5393
	TBT	6.4583	4.5477	4.0683	3.2755	6.4583	5.3073	4.6764	3.5157
	SBT	6.4588	4.5478	4.0680	3.2752	6.4588	5.3078	4.6767	3.5139
	Quasi-3D TBT	6.4615	4.5801	4.1098	3.2901	6.4615	5.3296	4.7159	3.5444
	Quasi-3D SBT	6.4638	4.5808	4.1097	3.2890	6.4638	5.3314	4.7166	3.5413
Classical	CBT	6.4657	4.5242	4.0613	3.3580	6.4657	5.2736	4.6294	3.6115
($l = 0$)	FBT	6.2021	4.3564	3.9073	3.1857	6.2021	5.0775	4.4667	3.4317
	TBT	6.2025	4.3518	3.8952	3.1651	6.2025	5.0801	4.4657	3.3909
	SBT	6.2029	4.3518	3.8949	3.1655	6.2029	5.0804	4.4659	3.3900
	Quasi-3D TBT	6.2085	4.3877	3.9406	3.1830	6.2085	5.1057	4.5091	3.4237
	Quasi-3D SBT	6.2107	4.3884	3.9406	3.1825	6.2107	5.1073	4.5097	3.4214

Table 10: Dimensionless fundamental frequencies of SiC/Al microbeams ($a/h = 10$)

h/l	Theory	Mori-Tanaka scheme				Classical rule of mixture			
		$p = 0$	0.5	1	10	$p = 0$	0.5	1	10
1	CBT	16.1966	11.7981	10.4765	7.5970	16.1966	13.7529	12.3671	8.2646
	FBT	15.8337	11.5436	10.2486	7.4084	15.8337	13.4558	12.1057	8.0624
	TBT	16.1144	11.7447	10.4344	7.5663	16.1144	13.6824	12.3095	8.2357
	SBT	16.1152	11.7449	10.4340	7.5647	16.1152	13.6837	12.3100	8.2341
	Quasi-3D TBT	16.0945	11.7428	10.4388	7.5587	16.0945	13.6728	12.3100	8.2363
	Quasi-3D SBT	16.0963	11.7432	10.4383	7.5559	16.0963	13.6747	12.3107	8.2330
2	CBT	9.8837	7.1113	6.3381	4.8071	9.8837	8.2867	7.3994	5.2101
	FBT	9.7550	7.0251	6.2598	4.7308	9.7550	8.1863	7.3134	5.1293
	TBT	9.8140	7.0661	6.2988	4.7702	9.8140	8.2316	7.3536	5.1723
	SBT	9.8144	7.0662	6.2985	4.7690	9.8144	8.2321	7.3539	5.1707
	Quasi-3D TBT	9.8072	7.0825	6.3231	4.7749	9.8072	8.2393	7.3747	5.1889
	Quasi-3D SBT	9.8087	7.0829	6.3227	4.7724	9.8087	8.2406	7.3751	5.1855
4	CBT	7.5185	5.3304	4.7722	3.8022	7.5185	6.2089	5.4955	4.1055
	FBT	7.4332	5.2751	4.7214	3.7474	7.4332	6.1445	5.4415	4.0479
	TBT	7.4479	5.2843	4.7292	3.7550	7.4479	6.1559	5.4510	4.0534
	SBT	7.4481	5.2844	4.7290	3.7544	7.4481	6.1561	5.4511	4.0523
	Quasi-3D TBT	7.4468	5.3125	4.7672	3.7676	7.4468	6.1733	5.4856	4.0810
	Quasi-3D SBT	7.4484	5.3128	4.7669	3.7655	7.4484	6.1745	5.4857	4.0779
8	CBT	6.7998	4.7827	4.2923	3.5063	6.7998	5.5696	4.9054	3.7792
	FBT	6.7238	4.7339	4.2474	3.4562	6.7238	5.5129	4.8581	3.7266
	TBT	6.7276	4.7352	4.2468	3.4537	6.7276	5.5163	4.8603	3.7192
	SBT	6.7277	4.7352	4.2466	3.4536	6.7277	5.5164	4.8604	3.7187
	Quasi-3D TBT	6.7285	4.7684	4.2908	3.4696	6.7285	5.5376	4.9007	3.7516
	Quasi-3D SBT	6.7301	4.7687	4.2906	3.4678	6.7301	5.5387	4.9008	3.7488
Classical	CBT	6.5444	4.5869	4.1211	3.4026	6.5444	5.3410	4.6937	3.6647
($l = 0$)	FBT	6.4713	4.5401	4.0780	3.3540	6.4713	5.2867	4.6484	3.6138
	TBT	6.4713	4.5387	4.0744	3.3477	6.4713	5.2874	4.6481	3.6013
	SBT	6.4714	4.5387	4.0743	3.3478	6.4714	5.2875	4.6482	3.6010
	Quasi-3D TBT	6.4731	4.5740	4.1209	3.3649	6.4731	5.3102	4.6909	3.6356
	Quasi-3D SBT	6.4747	4.5743	4.1207	3.3633	6.4747	5.3113	4.6910	3.6330

Table 11: Dimensionless critical buckling loads of SiC/Al microbeams ($a/h = 5$)

h/l	Theory	Mori-Tanaka scheme				Classical rule of mixture			
		$p = 0$	0.5	1	10	$p = 0$	0.5	1	10
1	CBT	368.9461	187.6062	144.7108	71.7514	368.9461	254.7402	201.5379	85.0019
	FBT	310.5978	160.9292	124.6102	61.7351	310.5978	218.6399	174.4544	73.1689
	TBT	354.1249	180.8209	140.0364	69.4318	354.1249	244.3914	194.0359	82.6019
	SBT	354.2790	180.8531	139.9959	69.3196	354.2790	244.5700	194.1098	82.4758
	Quasi-3D TBT	354.6933	181.4854	140.6387	69.5886	354.6933	245.1900	194.8498	82.8707
	Quasi-3D SBT	354.8704	181.5266	140.6068	69.4809	354.8704	245.3746	194.9271	82.7386
2	CBT	137.3900	68.1560	52.9616	28.7283	137.3900	92.4829	72.1428	33.7797
	FBT	124.0410	62.4722	48.6502	26.0529	124.0410	84.9125	66.7563	30.7010
	TBT	129.8802	64.7694	50.3920	27.0246	129.8802	87.6942	68.6522	31.8762
	SBT	129.9246	64.7767	50.3737	26.9727	129.9246	87.7416	68.6725	31.8019
	Quasi-3D TBT	130.4657	65.4449	51.0256	27.2470	130.4657	88.4632	69.4552	32.2157
	Quasi-3D SBT	130.5332	65.4602	51.0144	27.1995	130.5332	88.5192	69.4786	32.1388
4	CBT	79.5009	38.2935	30.0243	17.9726	79.5009	51.9186	39.7940	20.9741
	FBT	72.6931	35.3507	27.7292	16.2486	72.6931	48.0757	37.0774	19.0300
	TBT	73.8107	35.7506	27.9480	16.3030	73.8107	48.5182	37.3062	18.9845
	SBT	73.8277	35.7525	27.9396	16.2849	73.8277	48.5334	37.3131	18.9470
	Quasi-3D TBT	74.4088	36.4348	28.6071	16.5816	74.4088	49.2648	38.1008	19.3890
	Quasi-3D SBT	74.4489	36.4437	28.6041	16.5650	74.4489	49.2907	38.1105	19.3483
8	CBT	65.0287	30.8279	24.2899	15.2836	65.0287	41.7775	31.7068	17.7727
	FBT	59.5305	28.3968	22.3653	13.7366	59.5305	38.6308	29.4669	16.0395
	TBT	59.7916	28.4947	22.3291	13.5907	59.7916	38.7239	29.4697	15.6980
	SBT	59.8018	28.4953	22.3244	13.5877	59.8018	38.7311	29.4733	15.6806
	Quasi-3D TBT	60.3946	29.1822	22.9987	13.8927	60.3946	39.4618	30.2609	16.1306
	Quasi-3D SBT	60.4278	29.1895	22.9985	13.8894	60.4278	39.4804	30.2671	16.1090
Classical	CBT	60.2355	28.3553	22.3907	14.3930	60.2355	38.4188	29.0283	16.7124
$l = 0$	FBT	55.1416	26.0779	20.5767	12.8990	55.1416	35.4813	26.9291	15.0425
	TBT	55.1483	26.0913	20.4668	12.6871	55.1483	35.4799	26.8743	14.5981
	SBT	55.1562	26.0916	20.4636	12.6904	55.1562	35.4845	26.8767	14.5897
	Quasi-3D TBT	55.7531	26.7802	21.1405	12.9983	55.7531	36.2145	27.6641	15.0419
	Quasi-3D SBT	55.7841	26.7869	21.1415	13.0005	55.7841	36.2309	27.6692	15.0288

Table 12: Dimensionless critical buckling loads of SiC/Al microbeams ($a/h = 10$)

h/l	Theory	Mori-Tanaka scheme				Classical rule of mixture			
		$p = 0$	0.5	1	10	$p = 0$	0.5	1	10
1	CBT	368.9461	187.6062	144.7108	71.7514	368.9461	254.7402	201.5379	85.0019
	FBT	352.1681	181.6518	140.7797	70.6745	352.1681	246.8104	196.4931	83.6749
	TBT	365.0902	185.8471	143.5025	71.1508	365.0902	252.0480	199.5919	84.3826
	SBT	365.1289	185.8543	143.4906	71.1201	365.1289	252.0942	199.6102	84.3484
	Quasi-3D TBT	365.2609	186.3476	144.0387	71.2964	365.2609	252.5089	200.2057	84.6862
	Quasi-3D SBT	365.3251	186.3591	144.0274	71.2545	365.3251	252.5658	200.2241	84.6327
2	CBT	137.3900	68.1560	52.9616	28.7283	137.3900	92.4829	72.1428	33.7797
	FBT	133.7564	66.9790	52.2187	28.4424	135.4120	91.2251	71.2284	33.2761
	TBT	135.4120	67.2676	52.2877	28.2768	135.4120	92.0665	72.1670	34.0281
	SBT	135.4231	67.2690	52.2822	28.2618	135.4231	91.2374	71.2334	33.2548
	Quasi-3D TBT	135.5906	67.7727	52.8346	28.4424	135.5906	91.6763	71.8392	33.6002
	Quasi-3D SBT	135.6273	67.7781	52.8293	28.4166	135.6273	91.7002	71.8441	33.5612
4	CBT	79.5009	38.2935	30.0243	17.9726	79.5009	51.9186	39.7940	20.9741
	FBT	77.6747	37.5326	29.4777	17.5999	77.6747	51.0478	39.2441	20.5818
	TBT	77.9884	37.6202	29.4729	17.5202	77.9884	51.0193	39.1375	20.4337
	SBT	77.9926	37.6204	29.4703	17.5147	77.9926	51.0232	39.1391	20.4223
	Quasi-3D TBT	78.1731	38.1289	30.0290	17.7049	78.1731	51.4634	39.7459	20.7795
	Quasi-3D SBT	78.2029	38.1329	30.0261	17.6879	78.2029	51.4796	39.7473	20.7507
8	CBT	65.0287	30.8279	24.2899	15.2836	65.0287	41.7775	31.7068	17.7727
	FBT	63.5592	30.1209	23.7538	14.8710	63.5592	40.9803	31.1570	17.3377
	TBT	63.6316	30.2077	23.7665	14.8204	63.6316	40.9678	31.1147	17.2020
	SBT	63.6342	30.2078	23.7650	14.8193	63.6342	40.9696	31.1156	17.1965
	Quasi-3D TBT	63.8187	30.7180	24.3265	15.0136	63.8187	41.4092	31.7222	17.5582
	Quasi-3D SBT	63.8468	30.7216	24.3245	15.0005	63.8468	41.4236	31.7228	17.5351
Classical	CBT	60.2355	28.3553	22.3907	14.3930	60.2355	38.4188	29.0283	16.7124
($l = 0$)	FBT	58.8757	27.6617	21.8546	13.9655	58.8757	37.6400	28.4737	16.2613
	TBT	58.8765	27.7527	21.8761	13.9243	58.8765	37.6387	28.4576	16.1276
	SBT	58.8786	27.7526	21.8750	13.9252	58.8786	37.6399	28.4582	16.1249
	Quasi-3D TBT	59.0645	28.2635	22.4377	14.1211	59.0645	38.0791	29.0647	16.4883
	Quasi-3D SBT	59.0920	28.2670	22.4360	14.1096	59.0920	38.0929	29.0650	16.4678

Table 13: Dimensionless critical buckling loads of Al_2O_3/SUS304 microbeams ($a/h = 5$)

h/l	Theory	Mori-Tanaka scheme				Classical rule of mixture			
		$p = 0$	0.5	1	10	$p = 0$	0.5	1	10
1	CBT	102.9259	83.5272	75.8559	59.1987	102.9259	86.2293	78.3554	59.9323
	FBT	86.0687	69.9834	63.4828	49.2406	86.0687	72.2650	65.6283	49.8307
	TBT	98.5842	79.9966	72.7288	56.8378	98.5842	82.5560	75.0903	57.5577
	SBT	98.6269	80.0392	72.7542	56.8261	98.6269	82.6046	75.1226	57.5446
	Quasi-3D TBT	98.8844	80.2800	72.9823	56.9828	98.8844	82.8519	75.3618	57.7019
	Quasi-3D SBT	98.9519	80.3415	73.0273	56.9914	98.9519	82.9189	75.4128	57.7094
2	CBT	39.4784	31.7701	28.9964	23.2146	39.4784	32.7631	29.8462	23.5407
	FBT	35.3465	28.5139	25.9872	20.6480	35.3465	29.4140	26.7761	20.9276
	TBT	37.1259	29.9112	27.2953	21.7917	37.1259	30.8452	28.1034	22.0945
	SBT	37.1384	29.9236	27.3026	21.7872	37.1384	30.8593	28.1128	22.0891
	Quasi-3D TBT	37.4450	30.2020	27.5648	21.9705	37.4450	31.1459	28.3860	22.2751
	Quasi-3D SBT	37.4825	30.2338	27.5913	21.9847	37.4825	31.1792	28.4142	22.2887
4	CBT	23.6166	18.8309	17.2815	14.2186	23.6166	19.3965	17.7189	14.4429
	FBT	21.3975	17.1068	15.6747	12.7900	21.3975	17.6265	16.0893	12.9847
	TBT	21.7522	17.3858	15.9291	13.0070	21.7522	17.9144	16.3512	13.2026
	SBT	21.7573	17.3905	15.9320	13.0066	21.7573	17.9196	16.3549	13.2017
	Quasi-3D TBT	22.0851	17.6820	16.2104	13.2116	22.0851	18.2184	16.6420	13.4112
	Quasi-3D SBT	22.1151	17.7064	16.2323	13.2282	22.1151	18.2434	16.6645	13.4275
8	CBT	19.6511	15.5960	14.3528	11.9696	19.6511	16.0549	14.6871	12.1684
	FBT	17.8226	14.1831	13.0317	10.7765	17.8226	14.6054	13.3503	10.9494
	TBT	17.9069	14.2537	13.0859	10.8058	17.9069	14.6810	13.4120	10.9738
	SBT	17.9102	14.2565	13.0878	10.8071	17.9102	14.6841	13.4144	10.9747
	Quasi-3D TBT	18.2452	14.5519	13.3718	11.0206	18.2452	14.9863	13.7060	11.1935
	Quasi-3D SBT	18.2733	14.5745	13.3925	11.0381	18.2733	15.0093	13.7270	11.2109
Classical	CBT	18.3377	14.5247	13.3828	11.2247	18.3377	14.9481	13.6829	11.4151
$l = 0$	FBT	16.6307	13.2083	12.1505	10.1052	16.6307	13.5980	12.4371	10.2709
	TBT	16.6331	13.2162	12.1440	10.0760	16.6331	13.6101	12.4384	10.2348
	SBT	16.6358	13.2183	12.1456	10.0779	16.6358	13.6123	12.4403	10.2364
	Quasi-3D TBT	16.9734	13.5152	12.4316	10.2947	16.9734	13.9158	12.7335	10.4587
	Quasi-3D SBT	17.0009	13.5372	12.4520	10.3125	17.0009	13.9381	12.7542	10.4765

Table 14: Dimensionless critical buckling loads of Al_2O_3/SUS304 microbeams ($a/h = 10$)

h/l	Theory	Mori-Tanaka scheme				Classical rule of mixture			
		$p = 0$	0.5	1	10	$p = 0$	0.5	1	10
1	CBT	102.9259	83.5272	75.8559	59.1987	102.9259	86.2293	78.3554	59.9323
	FBT	98.0494	79.6160	72.2791	56.3044	98.0494	82.1976	74.6790	56.9953
	TBT	101.7940	82.6068	75.0413	58.5841	101.7940	85.2715	77.5047	59.3142
	SBT	101.8047	82.6177	75.0475	58.5804	101.8047	85.2840	77.5127	59.3101
	Quasi-3D TBT	101.8805	82.7116	75.1479	58.6325	101.8805	85.3772	77.6166	59.3645
	Quasi-3D SBT	101.9172	82.7432	75.1738	58.6446	101.9172	85.4106	77.6442	59.3763
2	CBT	39.4784	31.7701	28.9964	23.2146	39.4784	32.7631	29.8462	23.5407
	FBT	38.3462	30.8796	28.1725	22.5077	38.3462	31.8474	29.0063	22.8207
	TBT	38.8561	31.2789	28.5467	22.8374	38.8561	32.2563	29.3856	23.1573
	SBT	38.8592	31.2820	28.5484	22.8359	38.8592	32.2599	29.3880	23.1555
	Quasi-3D TBT	38.9498	31.3868	28.6592	22.8972	38.9498	32.3643	29.5020	23.2197
	Quasi-3D SBT	38.9790	31.4110	28.6805	22.9110	38.9790	32.3891	29.5238	23.2334
4	CBT	23.6166	18.8309	17.2815	14.2186	23.6166	19.3965	17.7189	14.4429
	FBT	23.0172	18.3661	16.8479	13.8307	23.0172	18.9195	17.2795	14.0468
	TBT	23.1180	18.4451	16.9200	13.8928	23.1180	19.0010	17.3536	14.1091
	SBT	23.1192	18.4463	16.9207	13.8925	23.1192	19.0024	17.3546	14.1087
	Quasi-3D TBT	23.2171	18.5555	17.0370	13.9616	23.2171	19.1108	17.4733	14.1813
	Quasi-3D SBT	23.2444	18.5778	17.0572	13.9762	23.2444	19.1335	17.4937	14.1959
8	CBT	19.6511	15.5960	14.3528	11.9696	19.6511	16.0549	14.6871	12.1684
	FBT	19.1591	15.2166	13.9976	11.6468	19.1591	15.6657	14.3279	11.8385
	TBT	19.1827	15.2363	14.0127	11.6548	19.1827	15.6869	14.3452	11.8450
	SBT	19.1835	15.2370	14.0132	11.6551	19.1835	15.6877	14.3458	11.8452
	Quasi-3D TBT	19.2839	15.3476	14.1315	11.7273	19.2839	15.7974	14.4661	11.9212
	Quasi-3D SBT	19.3108	15.3694	14.1513	11.7422	19.3108	15.8195	14.4861	11.9361
Classical	CBT	18.3377	14.5247	13.3828	11.2247	18.3377	14.9481	13.6829	11.4151
$l = 0$	FBT	17.8789	14.1716	13.0519	10.9222	17.8789	14.5861	13.3486	11.1058
	TBT	17.8792	14.1735	13.0497	10.9133	17.8792	14.5892	13.3487	11.0949
	SBT	17.8799	14.1741	13.0501	10.9138	17.8799	14.5898	13.3492	11.0953
	Quasi-3D TBT	17.9813	14.2852	13.1692	10.9872	17.9813	14.7000	13.4701	11.1726
	Quasi-3D SBT	18.0079	14.3068	13.1889	11.0022	18.0079	14.7220	13.4900	11.1876

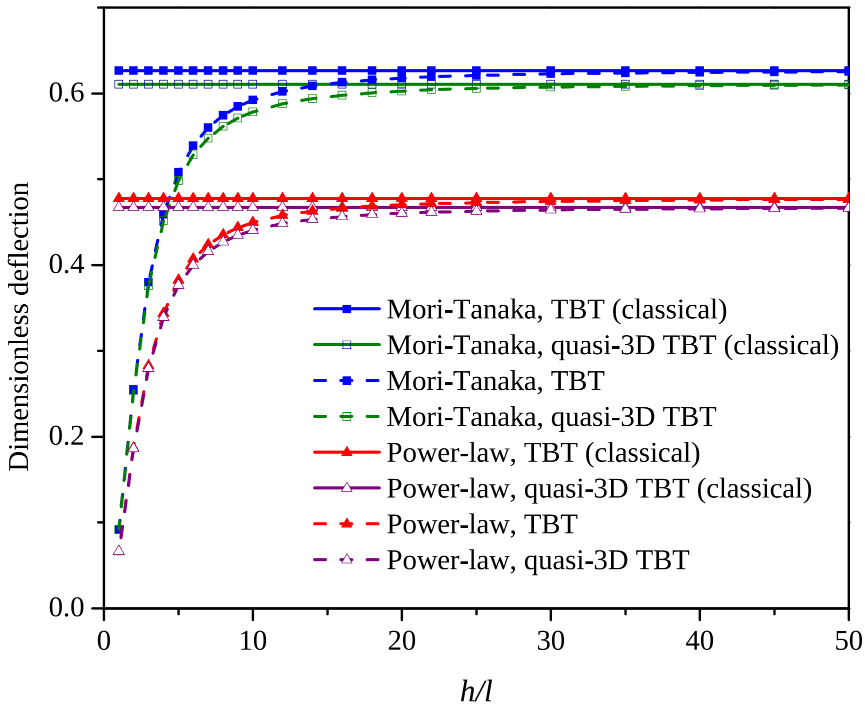

(a) $p = 1$.

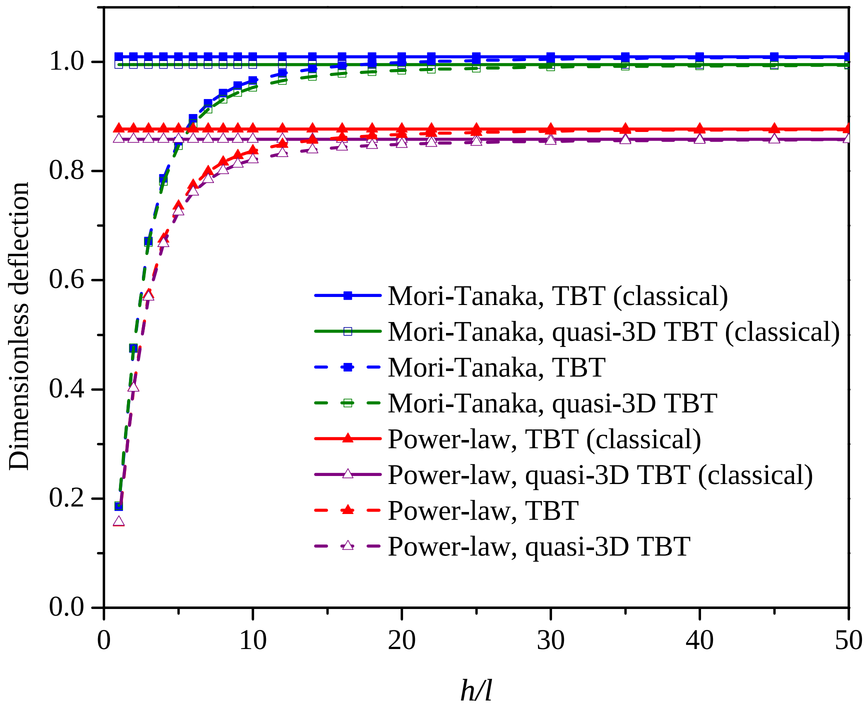

(b) $p = 10$.

Figure 1: Dimensionless maximum deflections of SiC/Al microbeams under uniform loads using TBT and quasi-3D TBT.

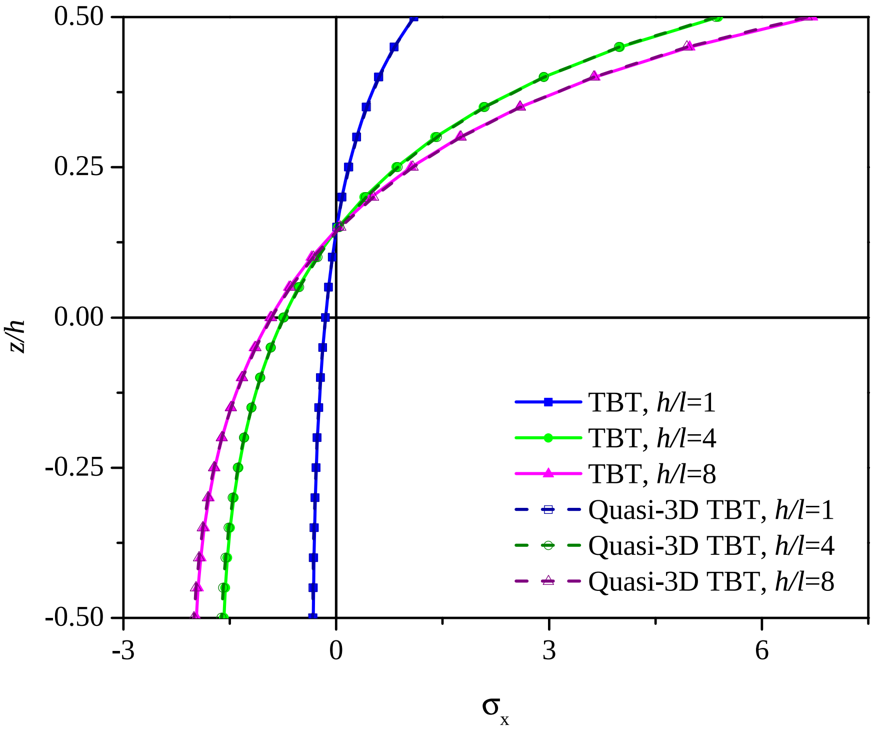

(a) $p = 1$.

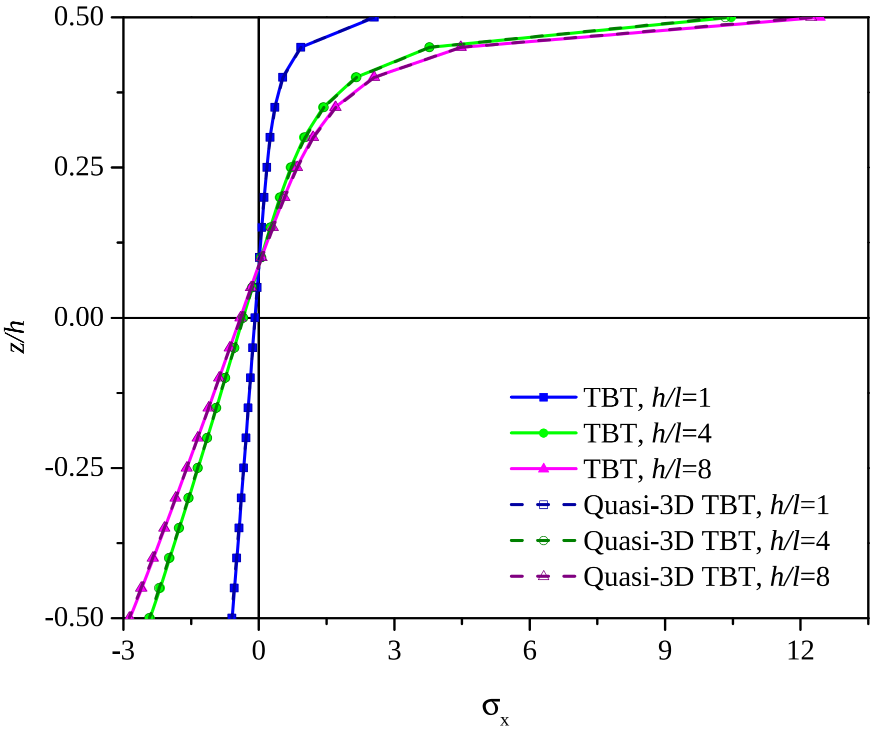

(b) $p = 10$.

Figure 2: Variation of $\sigma_x(a/2, z)$ through the depth using TBT and quasi-3D TBT (Mori-Tanaka scheme).

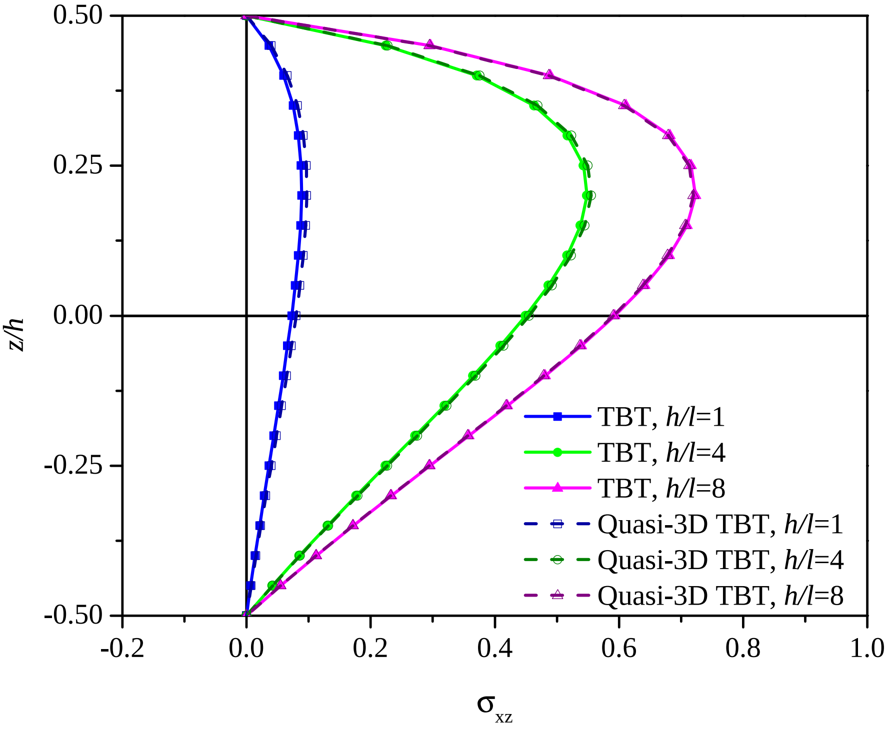

(a) $p = 1$.

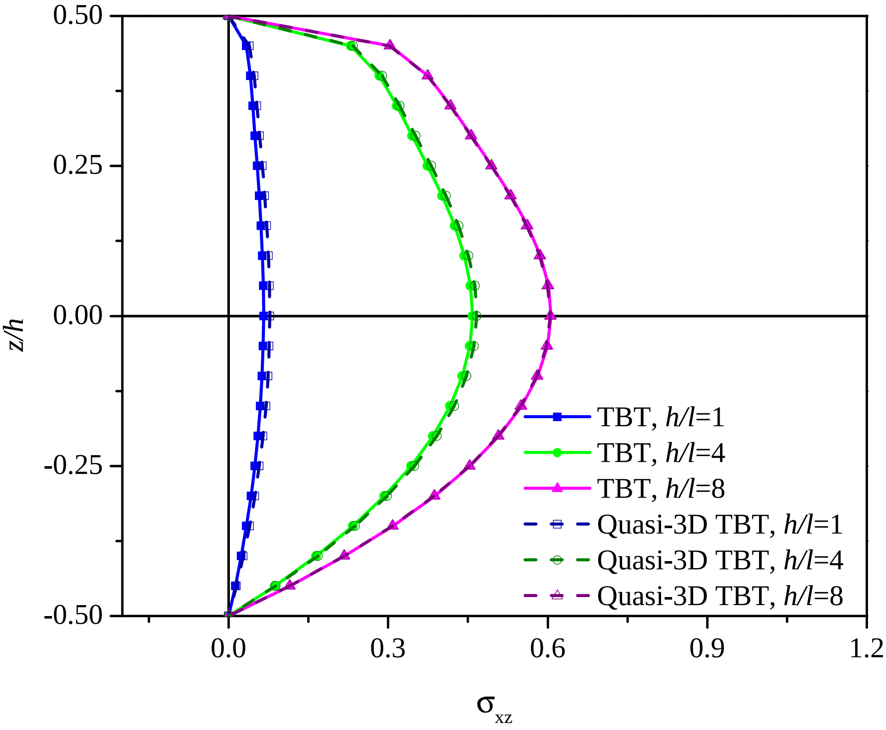

(b) $p = 10$.

Figure 3: Variation of $\sigma_{xz}(0, z)$ through the depth using TBT and quasi-3D TBT (Mori-Tanaka scheme).

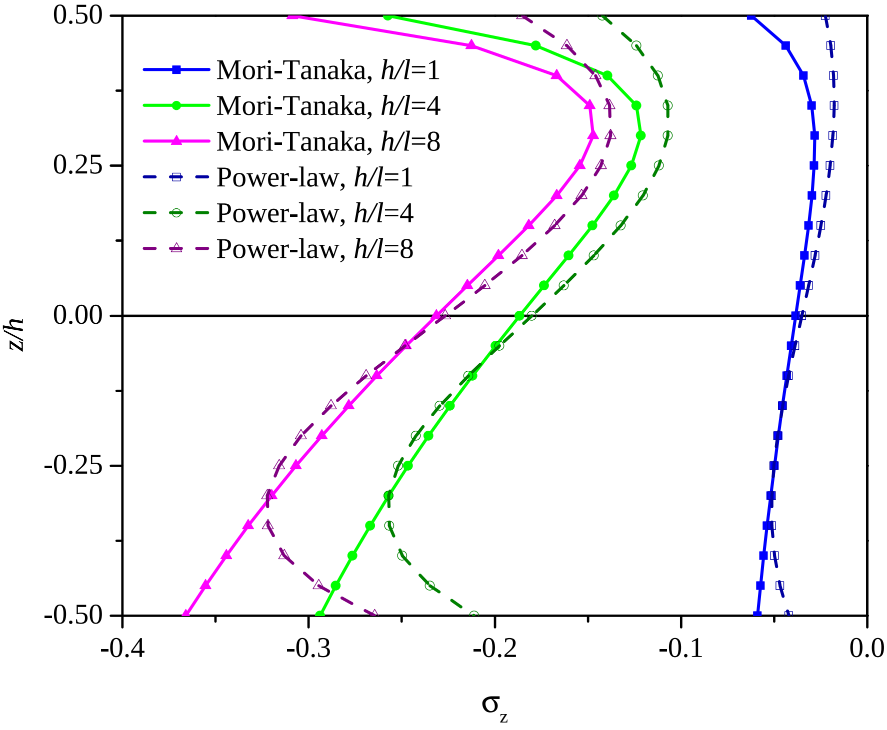

(a) $p = 1$.

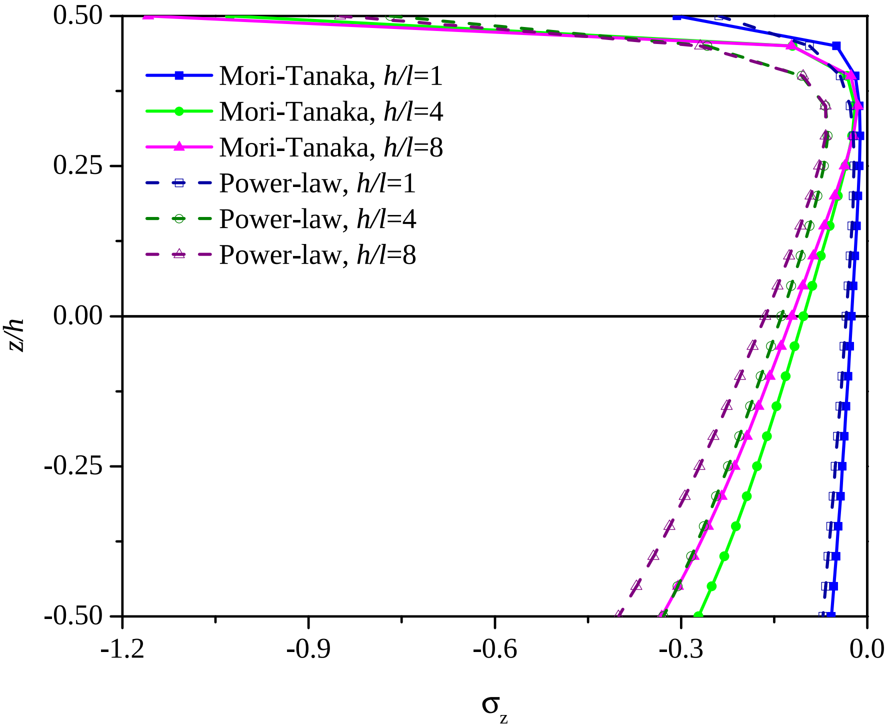

(b) $p = 10$.

Figure 4: Variation of $\sigma_z(a/2, z)$ through the depth using quasi-3D TBT.

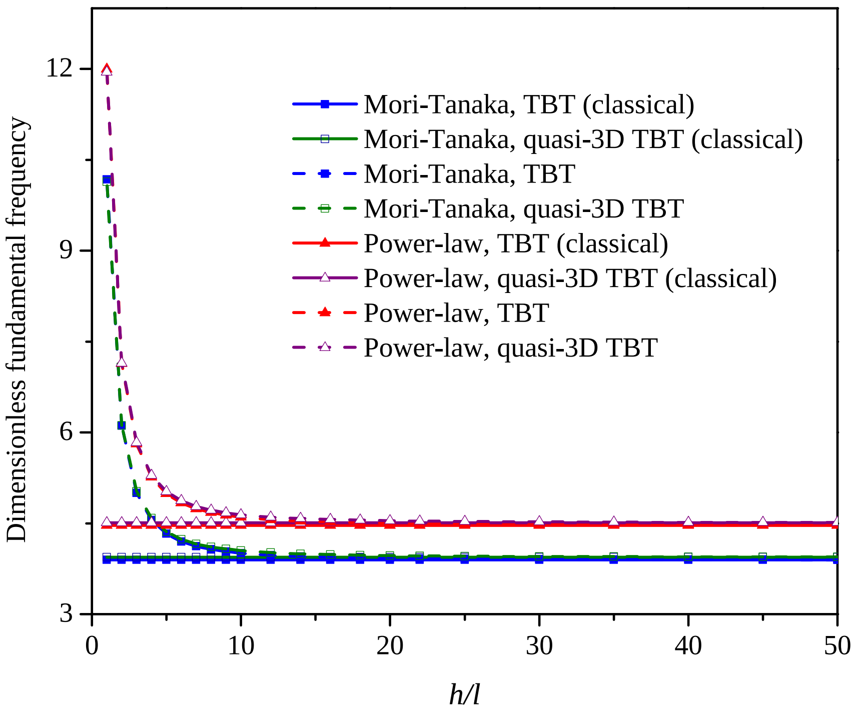

(a) $p = 1$.

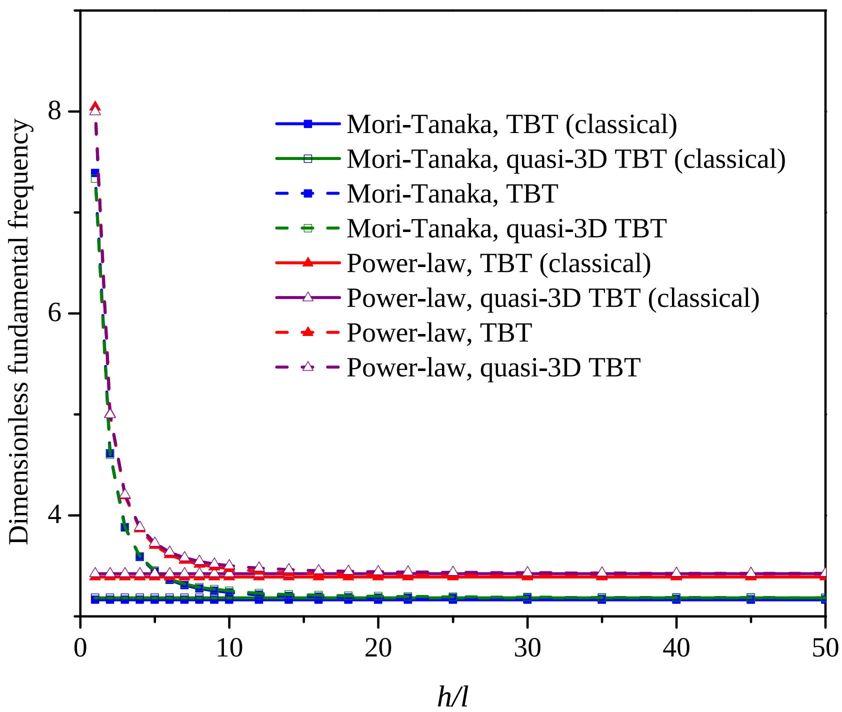

(b) $p = 10$.

Figure 5: Dimensionless fundamental frequencies of SiC/Al microbeams using TBT and quasi-TBT.

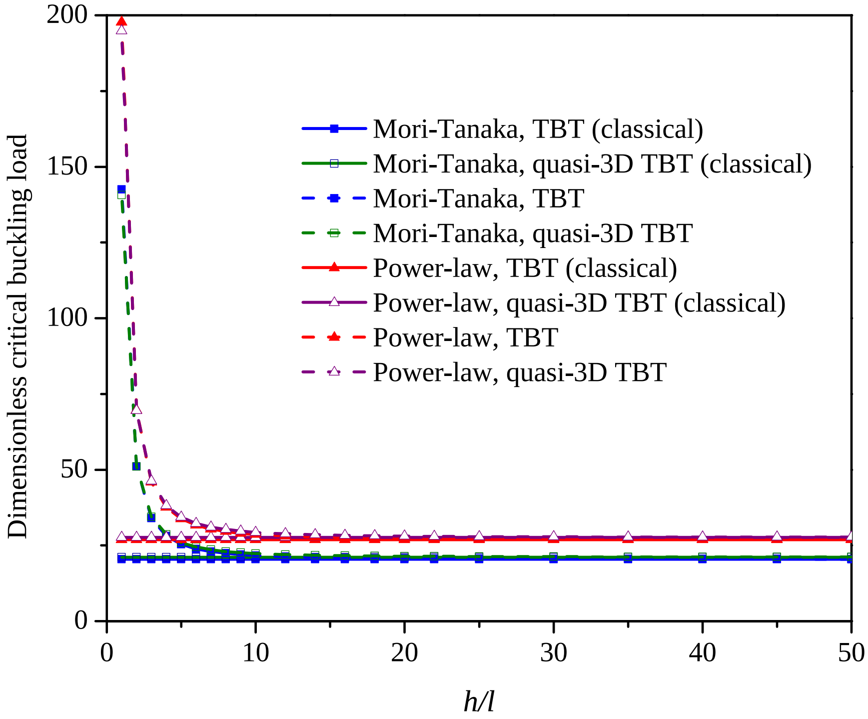

(a) $p = 1$.

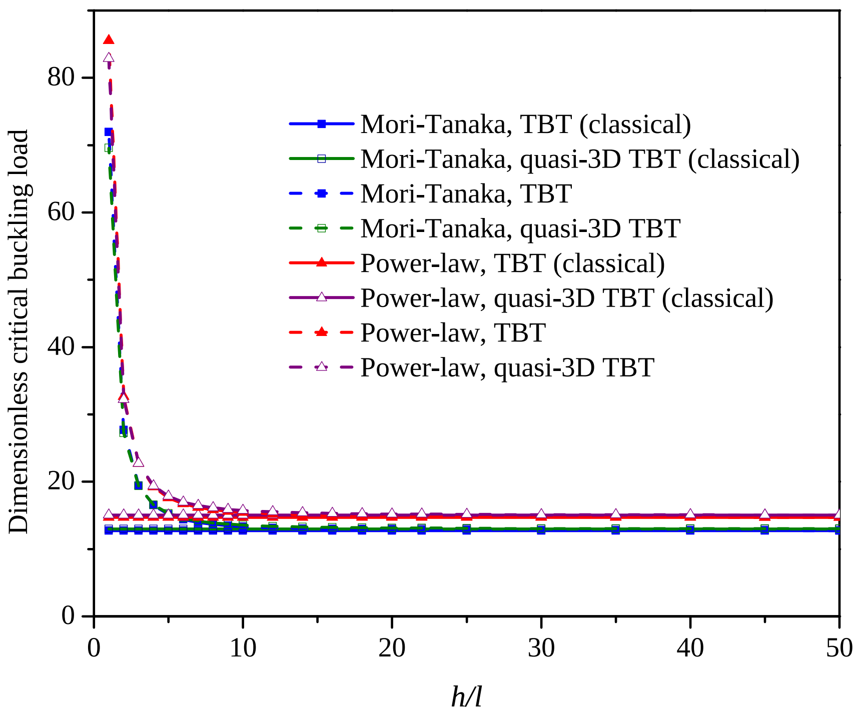

(b) $p = 10$.

Figure 6: Dimensionless critical buckling loads of SiC/Al microbeams using TBT and quasi-TBT.